Environment International 177 (2023) 108015

Contents lists available at ScienceDirect

Environment International

journal homepage: www.elsevier.com/locate/envint

Full length article

Transcriptomic profiling reveals differential cellular response to copper oxide nanoparticles and polystyrene nanoplastics in perfused human placenta

S. Chortarea [a], G. Gupta [a], L.A. Saarimäki [b], W. Netkueakul [a], P. Manser [a], L. Aengenheister [a,c], A. Wichser [d], V. Fortino [e], P. Wick [a], D. Greco [b,f], T. Buerki-Thurnherr [a,*]

[a] Laboratory for Particles-Biology Interactions, Swiss Federal Laboratories for Materials Science and Technology (Empa), 9014 St. Gallen, Switzerland
[b] Finnish Hub for Development and Validation of Integrated Approaches (FHAIVE), Faculty of Medicine and Health Technology, Tampere University, Tampere, Finland
[c] Human Biomonitoring Research Unit, Department of Precision Health, Luxembourg Institute of Health (LIH), 1 A-B, Rue Thomas Edison, L-1445 Strassen, Luxembourg
[d] Laboratory for Advanced Analytical Technologies, Empa, Swiss Federal Laboratories for Materials, Science and Technology, Dübendorf, Switzerland
[e] Institute of Biomedicine, School of Medicine, University of Eastern Finland, Kuopio, Finland
[f] Institute of Biotechnology, University of Helsinki, Helsinki, Finland

ARTICLE INFO

Handling Editor: Marti Nadal

Keywords:
Nanoplastics
CuO nanoparticles
Placenta
Transcriptomic profiling
Developmental toxicity pathways

ABSTRACT

The growing nanoparticulate pollution (e.g. engineered nanoparticles (NPs) or nanoplastics) has been shown to pose potential threats to human health. In particular, sensitive populations such as pregnant women and their unborn children need to be protected from harmful environmental exposures. However, developmental toxicity from prenatal exposure to pollution particles is not yet well studied despite evidence of particle accumulation in human placenta. Our study aimed to investigate how copper oxide NPs (CuO NPs; 10–20 nm) and polystyrene nanoplastics (PS NPs; 70 nm) impact on gene expression in *ex vivo* perfused human placental tissue. Whole genome microarray analysis revealed changes in global gene expression profile after 6 h of perfusion with sub-cytotoxic concentrations of CuO (10 μg/mL) and PS NPs (25 μg/mL). Pathway and gene ontology enrichment analysis of the differentially expressed genes suggested that CuO and PS NPs trigger distinct cellular response in placental tissue. While CuO NPs induced pathways related to angiogenesis, protein misfolding and heat shock responses, PS NPs affected the expression of genes related to inflammation and iron homeostasis. The observed effects on protein misfolding, cytokine signaling, and hormones were corroborated by western blot (accumulation of polyubiquitinated proteins) or qPCR analysis. Overall, the results of the present study revealed extensive and material-specific interference of CuO and PS NPs with placental gene expression from a single short-term exposure which deserves increasing attention. In addition, the placenta, which is often neglected in developmental toxicity studies, should be a key focus in the future safety assessment of NPs in pregnancy.

1. Introduction

The growing fetus is highly vulnerable to harmful substances even at concentrations that are not of any concern for adults. In order to protect the developing fetus from possible adverse health effects, the main role of the placenta is to act as a protective barrier for the entry of harmful substances. However, epidemiological, animal and human *in vitro/ex vivo* studies provide increasing evidence that environmental particles (e.g. micro/nanoplastics, particulate matter and engineered nanomaterials (NMs) such as gold (Au), silica (SiO_2), silver (Ag), titanium oxide (TiO_2)) are able to overcome this barrier and reach fetal tissues, raising concerns on possible pregnancy or fetal complications (Fournier, 2020; Fleischer, 2014; Aengenheister, 2018; Vidmar, 2018; Yamashita, 2011; Aengenheister, 2019). Moreover, besides forming a protective barrier, the placenta performs many additional functions indispensable towards successful pregnancy including maternal-fetal exchange of nutrients, gases and waste products as well as essential endocrine, immunologic and metabolic functions (Burton and Fowden, 2015). Therefore, even in the absence of placental translocation, NMs such as carbon nanotubes (CNTs) or TiO_2, may still pose risks to fetal development if they interfere with the functionality of the placental tissue and/or through the release of placental mediators (Huang, 2014; Notter, 2018; Dugershaw, 2020;

* Corresponding author at: Empa, Lerchenfeldstrasse 5, 9014 St. Gallen, Switzerland.
E-mail address: tina.buerki@empa.ch (T. Buerki-Thurnherr).

https://doi.org/10.1016/j.envint.2023.108015
Received 10 February 2023; Received in revised form 31 May 2023; Accepted 1 June 2023
Available online 7 June 2023

Buerki-Thurnherr, 2018). A hostile gestational environment for embryo-fetal development could not only lead to complications in pregnancy but may increase the risk for the development of diseases in later life, a concept known as the Barker hypothesis or developmental origin of health and disease (DOHaD) (Nobile et al., 2022; Hoffman et al., 2017).

With the rapid development in nanotechnology in recent years, various types of novel NMs with unique properties and innovative functions have been widely applied in areas of medicine, technology, electronics, cosmetics, and food manufacturing (Marchesan and Prato, 2013; Klębowski, 2018; Rashidi and Khosravi-Darani, 2011; Raj, 2012; Kamyshny and Magdassi, 2014). However, there is limited knowledge on the toxicological health risks of NMs, in particular for highly sensitive populations, such as pregnant women and the unborn children.

One of the most abundant and highly utilized types of engineered NMs are metal oxides with a production scale of thousands of tons per year (Landsiedel, 2010). Among metal oxides, copper oxides (CuO) are appealing due to their unique features regarding electrical, optical, magnetic and biocidal properties. Consequently, CuO NPs are manufactured for a variety of industrial and consumer applications such as electronic equipment, solar cells, lithium batteries, paints, processed wood, and plastics (Grigore, 2016). In addition, copper is found in particulate matter e.g. from power stations, smelters, metal foundries as well as in particles torn from asphalt and rubber tires (Midander, 2009; World Health Organization, 1998). The antimicrobial properties of CuO NPs have been or are expected to be applied in food packaging, wound dressings, skin products and textiles (Grigore, 2016; Honarvar et al., 2016; Das and Baker, 2016). Additional potential applications are as anti-cancer and bioimaging agents (Gnanavel et al., 2017). Hence, the annual production size of CuO NPs is rising and expected to reach 1600 tons by the year 2025 (Future Markets Inc.). As a result, these NPs have high potential to be released into the environment and enter the human body through effluent, consumer products, or improper disposal. While various studies have provided evidence that CuO NPs are particularly potent to provoke adverse effects in several organs in comparison to other metal oxide NPs (Di Bucchianico, 2013; Costa, 2018; Sarkar, 2011), limited information is available for the potential health risks during pregnancy. Copper is an essential trace element for numerous biological processes and deficient or excess copper levels have been linked to pregnancy complications such as preeclampsia (Fan et al., 2016; Song, 2017; Walker et al., 2011). Considering that systemic NPs tend to accumulate and persist in placental tissue (Aengenheister, 2018; Yamashita, 2011; Aengenheister, 2019), further studies are warranted to identify if CuO NPs can interfere with placental functions essential to embryo-fetal development.

Synthetic polymers and in particular plastics are another significant class of materials that cover a broad range of attractive characteristics and thus have a crucial impact in our daily life. Because of manifold applications, the production of plastics has significantly increased over the past 60 years to a global production of 348 million tons in 2017 (Plastics Europe, 2018). About 80 % of plastics are not properly recycled ending up in the environment or landfills, where they can start to degrade into highly persistent plastic particles in micro- (microplastics) and nano-dimensions (nanoplastics). The contamination with micro- and nanoplastics has been reported in water and air samples from all around the globe, therefore making it a serious environmental and human health concern (Lehner, 2019). Recently, micro- and nanoplastics have been observed in human lungs (Jenner, 2022), blood (Leslie, 2022), stool (Schwabl, 2019) and placenta (Ragusa, 2021; Braun, 2021; Ragusa, 2022). Moreover, there is indication that at least nanosized PS particles could reach the unborn child from *ex vivo* human placenta perfusion studies or inhalation studies in pregnant mice (Fournier, 2020; Wick, 2010). Recently, polyethylene terephthalate (PET) and polycarbonate (PC) microplastics have been detected in meconium, which further supports the hypothesis of placental uptake and fetal transfer of microplastics in humans (Zhang, 2021). While knowledge on the toxicity of micro- and nanoplastics in placental and fetal tissues is minimal, their presence in liver and intestine has been recently associated with liver cirrhosis and inflammatory bowel disease (IBD) (Yan, 2022; Horvatits, 2022). On the cellular level, the few existent studies are contradictory as some showed that nanoplastics are taken up and induce oxidative stress and/or pro-inflammatory responses in human cell lines, while other sreported the absence of toxic effects (reviewed in (Lehner, 2019; Hesler, 2019). Overall, there is an urgent need to better understand the developmental toxicity of nanoplastics including potential toxicity pathways in placental and fetal tissues.

In this study, we aimed to investigate the possible impact and differential response of CuO and PS NP exposure on the human placenta due to its central position and numerous indispensable functions at the interface between the mother and the developing child. A particular focus was set to unravel novel toxicity mechanisms at the molecular level using an unbiased whole genome transcriptomics profiling to unveil effects that might not readily be captured by traditional toxicity assays. Taking into account that the placenta is the most species-specific organ with substantial differences in placental development, structure and function between the species, we have utilized an ethically accepted and well established *ex vivo* human placenta perfusion model that closely resembles the *in vivo* situation (Aengenheister, 2021). The obtained human-relevant insights on placenta-mediated developmental toxicity pathways will support the protection of pregnant women as well as the safe design and use of engineered NMs.

2. Materials and methods

2.1. Chemicals and reagents

All chemicals and reagents used were obtained from Sigma-Aldrich (Switzerland), unless otherwise stated.

2.2. Nanoparticles (NPs)

CuO NPs were obtained from PlasmaChem, Germany within the EU FP7 Nanosolutions consortium (https://www.nanosolutions.eu). PS NPs of 70 nm primary size were commercially available (aqueous dispersion; 10 mg/mL) from Spherotech Inc. (FP-00552–2, Lucerne, Switzerland).

2.3. Dispersion preparation

CuO NPs were provided as powder and PS NPs as an aqueous suspension (1% w/v suspension in 0.02% sodium azide as preservative). CuO NP powder was dispersed in endotoxin-free water to a stock suspension of 1 mg/mL. The suspension was sonicated for 5 min using a probe sonicator (6 mm probe; Branson Sonifier 250, Branson Ultrasonic Co., Danbury, CT, USA) at a power output of 13 W, operating at 230 V/50 Hz. Aqueous suspension of PS NPs was vortexed before each use and immediately diluted in ultrapure water to obtain a stock dispersion of 1 mg/mL. Further dilutions of CuO and PS NPs to the required concentrations were prepared either in perfusion medium (PM) (*ex vivo* perfusions) or in supplemented cell culture medium (*in vitro* experiments). CuO NP stock suspensions were freshly prepared prior to the experiments, diluted to the working concentrations shortly after sonication and used immediately to avoid potential dissolution of CuO NPs.

2.4. Characterization of NPs

The morphology of CuO NPs was characterized using a scanning electron microscope (SEM) (Nova NanoSEM 230). SEM samples were coated with a 10 nm platinum layer to improve electrical conductivity. Images were taken at working distance of ~ 5 mm, at 20 kV, and in secondary electron mode. The zeta potential and hydrodynamic size distribution of both NP types was reported using a Zetasizer (Nano ZS, Malvern Instruments, Worcestershire, UK). NP stock suspensions were prepared as described before and were further diluted to 100 μg/mL in

ddH_2O and PM. Measurements (three consecutive measurements with a minimum of 15 runs of 10 s each) were performed at 25 °C at a detection angle of 90° using a He-Ne laser operating at a wavelength of 633 nm. The mean Z average (Zave) size was obtained from three separate measurements. The CuO surface area, endotoxin content and ion release was studied by Muoth *et al.*, using different analytical methods (Muoth, 2016). Characterization of PS NPs (SEM, hydrodynamic diameter and zeta potential in 10% PBS) was performed in a previous study (Aengenheister, 2018). A summary of the NP characteristics can be found in SI Table 1.

2.5. Ex vivo placental perfusion

Placentas were obtained from uncomplicated term pregnancies after caesarean section at the Cantonal Hospital and the Klinik Stephanshorn in St Gallen (Switzerland) with written informed consent from the expecting mothers prior to delivery. The study was approved by the local ethics committee (EKOS 10/078; PB-2018–00069) and performed in accordance with the principles of the Declaration of Helsinki. The placental perfusion experiments were performed on a human *ex vivo* dual recirculating human placental perfusion system, as described previously (Grafmueller, 2013, 2015; Wick, 2010). The perfusion medium (PM) consisted of M199 tissue culture medium, diluted 1:2 with Earl's buffer and supplemented with glucose (1 g/L), bovine serum albumin (BSA; 10 g/L), dextran 40 (10 g/L), sodium heparin (2500 IU/L), amoxicillin (250 mg/L) and sodium bicarbonate (2.2 g/L). The main criteria for successful perfusions were: (i) no observed leakage during the pre-perfusion of the tissue, (ii) <4 mL/h leakage from fetal to maternal circulation and (iii) stable pH during the experiment (7.2–7.4). After establishing the system, CuO and PS NPs were added to the maternal chamber to a final concentration of 10 and 25 μg/mL, respectively. For the transcriptomic analysis the perfusion experiments were performed in triplicates (n = 3) for both CuO and PS particles. Control perfusions with PM without addition of NPs (n = 2) were also conducted to obtain the baseline data. The sex of all placental samples used for microarray analysis (control- and NP-perfused) was female. Placenta tissue samples (~3 × 3 × 3 mm) from the villous region (from the middle of perfused tissue and avoiding the chorionic plate) were collected before (0 h; non-perfused cotyledon) and after 6 h of perfusion and stored in RNAlater stabilization solution (ThermoFisher Scientific, Zurich, Switzerland) at − 20 °C for the transcriptomic responses.

2.6. Toxicity assessment in human placental trophoblasts

The human placental choriocarcinoma cell line BeWo b30 was kindly provided by Prof. Dr. Ursula Graf-Hausner (Zurich University of Applied Science) with permission from Dr. Alan L. Schwartz (Washington University School of Medicine, MO, USA). BeWo cells were cultivated in trophoblast medium (TM), which is Ham's F-12 K medium (Gibco, Luzern, Switzerland) supplemented with 10% fetal calf serum (FCS, Invitrogen, Basel, Switzerland), 1% penicillin/streptomycin (Gibco, Luzern, Switzerland) and 2 mM L-Glutamine (Gibco, Luzern, Switzerland). Cells were sub-cultured at approximately 80–90% confluency twice a week using trypsin-EDTA solution and cultivated in a humidified incubator at 37 °C with 5% CO_2 atmosphere.

For cell viability assessment, BeWo cells were seeded in a 96-well plate at a density of 1×10^4 cells per well (three replicates were done per condition and experiment) and grown overnight under standard growth conditions. Subsequently, the cells were treated for 6 and 24 h with supplemented TM containing increasing concentrations of CuO NPs (concentration range: 0–50 μg/mL). Cadmium sulphate ($CdSO_4$) was applied as the positive control at a concentration of 1000 μM. Cells without treatment were used as negative control. CellTiter96® AQueous One Solution (Promega, Dübendorf, Switzerland) containing MTS (3-(4,5-dimethylthiazol-2-yl)-5-(3-carboxymethoxy-phenyl)-2-(4-sulfophenyl)–2H) as a water-soluble tetrazolium compound was used to assess the cellular metabolic activity. Optical density (OD) was measured at 490 nm with a microplate reader (Mithras2 Plate reader, Berthold Technologies, Germany) after incubating the cells with the MTS reagent at standard cell culture conditions for 60 min, according to the manufacturer's protocol. OD values were blank-corrected and normalized to untreated controls. PS NP toxicity assessment has been performed in a previous study (Aengenheister, 2018).

2.7. DNA microarrays

Total RNA was isolated from tissue lysates with miRNeasy Mini Kit according to manufacturer's instructions (Qiagen, GmbH, Hilden, Germany). RNA quantity and quality were assessed by NanoDrop (ND-1000, Thermo Fisher Scientific Inc., Wilmington, NC, USA) and Agilent Bioanalyzer 2100 (Agilent Technologies, Santa Clara, CA), respectively. RNA samples with RNA integrity number (RIN) > 7.5 were included in the microarray analysis.

cRNA synthesis was performed (from 100 ng of each independent RNA sample) using the Agilent Quick Amp, two-color microarray-gene expression labelling kit following the manufactureŕs instructions (Agilent Technologies, Santa Clara, USA). cRNAs were labelled with Cy3 or Cy5 dyes (Agilent Technologies, Santa Clara, USA), purified, and hybridized to Agilent SurePrint G3Human GE 8x60K DNA microarrays, for 17 h at 65 °C. Slides were washed and scanned with Agilent Microarray scanner G2505C (Agilent Technologies, Santa Clara, USA) and data (raw intensity values) were extracted with Agilent Feature Extraction software V11.5.1.1 (Agilent Technologies, Santa Clara, USA).

Microarray data associated with this publication have been deposited to the NCBI Gene Expression Omnibus (GEO) database and are accessible through the accession number GSE220756.

2.8. Data processing and differential expression analysis

Raw data processing and differential expression analysis were performed with *eUTOPIA* (Marwah, 2019), as described in (Kooter, 2019). Briefly, after importing raw files, quality control of the raw data was performed with the arrayQualityMetrics R package integrated in the platform. Signal intensity and background corrections were carried out by the quantile normalization method. Batch effects arising from the labeling and array-specific variances were corrected using the ComBat method from the R package sva (Leek, 2012), and probes mapped to the same gene symbol were aggregated using their median values. Finally, differentially expressed genes were identified using the R package limma which implements linear models and empirical Bayes statistics for differential expression (Ritchie, 2015). Variables used in the batch effect correction (*i.e.* dye, array) were included as covariates in the *limma* model together with the donor variable. Genes with nominal p-value < 0.01 and absolute log 2 fold change (logFC) > 1 (corresponding to 2-fold change in the linear scale) were considered statistically significant and used for further analyses. Hierarchical clustering was also performed with *eUTOPIA*.

2.9. Gene set functional enrichment analysis

Gene ontology based identification of overrepresented biological processes was carried out using Enrichr (Chen, 2013) enrichment analysis tool. FunMappOne (Scala, 2019) was used to summarize lists of gene ontology (GO) terms as well as for pathway analysis. INfORM (Inference of NetwOrk Response Modules) was applied to detect, evaluate and select gene modules with high statistical and biological significance (Marwah, 2018).

Venn diagrams were generated with Venny 2.1.0 (Oliveros). Alternatively, identification and visualization of biological networks from predicted enriched gene functions was carried out by the web-based GeneMANIA platform. In addition, visualization of the interactions among the proteins encoded by highly deregulated DEGs in both

treatments was performed using the web-based Search Tool for the Retrieval of Interacting Genes (STRING) prediction platform (Szklarczyk, 2017).

2.10. mRNA expression in placenta tissue

Verification of the expression of selected genes from the microarray analysis by qPCR was performed in a new set of placental perfusions (n = 3 each for CuO NPs, PS NPs and plain PM). The sex of the placentas were: controls – 3 males; PS NPs – 2 females; 1 male, CuO NPs – 3 females. Placenta samples were disrupted and homogenized in 0.7 mL of QIAzol Lysis Reagent (Qiagen, Hilden, Germany) using the TissueRuptor II (Qiagen, Hilden, Germany). The RNA extraction was performed following the instructions provided by the miRNeasy Mini Kit (Qiagen, Hilden, Germany). The RNA concentration and purity were determined by a NanoDrop ND-1000 spectrophotometer (Thermo Scientific, Witec AG, Littau, Switzerland) at 260 and 280 nm, considering a 260/280 ratio of 1.9–2.1 as pure RNA. The reverse transcriptase reactions were performed using the iScript cDNA synthesis Kit (BioRad, Cressier, Switzerland), following the manufacturer's protocol. Real-time PCR was carried out in a C1000™ Thermal Cycler using the iQ™ SYBR Green Supermix (BioRad, Cressier, Switzerland) as a reporter dye in accordance with the manufacturer's instructions. The primer sequences for all tested genes can be found in the SI Table 2. In addition, the following pre-validated PrimePCR™ primers (BioRad) for LPN2 (Unique assay ID: qHsaCED0045408), Cyp1A1 (Unique assay ID: qHsaCED0057334), Cyp1B1 (Unique assay ID: qHsaCED0057022), SLC11A2 (Unique assay ID: qHsaCED0043338), SLC40A1 (Unique assay ID: qHsaCED0005662) were used following the established validated protocols from the manufacturer. Relative expression of the genes was calculated after normalization to the internal standard gene Glyceraldehyde-3-phosphate dehydrogenase (*GAPDH*), using the ΔΔCt method as described by Schmittgen *et al.* (Schmittgen and Livak, 2008).

2.11. Western blot

For western blot, approx. 10 mg of tissue from control and CuO NPs (10 μg/mL) perfused placenta was collected and lysed by pulse homogenization for 30 sec in a RIPA buffer. Protease- and phosphatase inhibitors (HaltTM Protease Inhibitor Cocktail, Thermo Fisher Scientific; 1 mM PMSF (phenylmethylsulfonyl fluoride)) were freshly added to the RIPA buffer. Next, tissue lysates were centrifuged at 13000 × g for 15 min and supernatants were collected. The protein concentration was measured using the Bradford assay kit (Thermo Fisher Scientific) and 30 μg were loaded with sample buffer into each well of a NuPAGE 4–12% Bis–Tris gradient gel (Thermo Fisher Scientific). The polyubiquitinated proteins in SDS-PAGE were separated under non-reducing conditions by excluding DTT. Following electrophoretic separation, proteins were transferred to an Immobilon®-FL PVDF membrane (Millipore), blocked for 1 h in 3% BSA, and incubated overnight at 4 °C with primary antibodies against ubiquitin (dilution 1:2000, Catalog # PA3-16717, Invitrogen). HRP conjugated goat anti-rabbit antibody (Invitrogen, Germany) was used as a secondary antibody. HRP-conjugated mouse anti-beta-actin (dilution 1:2000; Thermo Fisher Scientific) was used as a loading control. The membrane was probed with SuperSignal™ West Dura Extended Duration Substrate (Thermo Fisher Scientific) and proteins were detected using the ChemiDoc-It imaging system (UVP).

2.12. Statistical analysis

The viability and gene expression results are expressed as mean ± standard deviation (SD) of three independent experiments (n = 3). Statistical comparison between groups was evaluated by unpaired Student's *t*-test (western blot and viability data) and one-way analysis of variance (ANOVA) followed by Dunnett's multiple comparison test analysis (qPCR data) using Graph Pad Prism (GraphPad Software Inc., La Jolla, CA, USA). A statistical significance was defined as $p < 0.05$ compared to the negative control group, with $p < 0.05$ and $p < 0.01$ represented as * and **, respectively.

3. Results and discussion

3.1. Characterization of CuO and PS NPs

The basic characteristics of CuO and PS particles are summarized in SI Figure 1 and SI Table 1. According to the provider and based on TEM/SEM image analysis in our previous publications, the primary particle size of CuO NPs was 20 nm, and for PS NPs 70 nm (Muoth, 2016; Aengenheister, 2018). However, SEM images revealed that agglomerates were formed for both CuO and PS particles when dispersed in water. Indeed, the scanning electron microscopy (SEM) micrographs of the CuO (dispersed in perfusion medium) showed agglomerates of micrometer-sized particles (SI Figure 1A). In accordance with the SEM images, hydrodynamic diameter measurements showed larger agglomerates of 1470 nm (±106.2) or 3629 nm (±428.2) formed when CuO NPs were suspended in water or PM, respectively (SI Figure 1B). Similarly, in PS suspensions, smaller agglomerates of 117 nm (±2) were observed when suspended in water, whereas larger assemblies of 501 nm (±18.5) occurred when dispersed in PM. The presence of larger particle agglomerates when PM was used as dispersion agent was further highlighted by the high polydispersity index (PDI; 0.564 and 0.577 for CuO and PS, respectively). In water the PDI was far lower for both materials tested (0.372 for CuO and 0.225 for PS). The observed agglomeration of PS NPs and CuO NPs in PM will likely impact on placental translocation and effects. For instance, we have previously shown that PS NP translocation across the placenta is size-dependent (Wick, 2010) and that NP agglomeration/aggregation can affect toxicity (Bruinink et al., 2015). The CuO NPs presented a negative surface charge of −36.5 mV (±1.4) in water. The surface charge for PS NPs in water was determined at −25 mV (±1.35). Both NP types were tested for endotoxin contamination and found endotoxin free (<0.5 EU ml/L). Other key physicochemical characteristics of CuO (e.g., BET specific surface, CuO dissolution) have been previously described by Mouth *et al.* (Muoth, 2016) and are summarized in SI Table 1.

3.2. Cytotoxicity and placental translocation of CuO and PS NPs

The effects of different CuO NP concentrations (0–50 μg/mL) on the cellular mitochondrial activity were assessed after 6 h and 24 h exposure on BeWo cells, an immortalized human trophoblastic cell line. These cells were selected as a model of the syncytiotrophoblasts, which are the first cells in contact with NPs in the *ex vivo* placental perfusion system. As shown in SI Figure 2, CuO NPs did induce a dose-dependent reduction in cell viability of trophoblasts after both 6 h (significant only at the highest concentrations of 25–50 μg/mL) and 24 h time points, with a dramatic cell loss at the 24 h treatment (significant at concentrations of 6.25–50 μg/mL). In accordance with our findings, CuO NPs induced major cytotoxicity on trophoblasts, in both 2D and 3D settings (Muoth, 2016; Zhang, 2018). It is conceivable that toxicity is at least partly mediated by Cu ions and we have observed dissolution of our CuO NPs in medium (13% after 10 min and 59% after 24 h) in our previous study (Muoth, 2016). Karlsson et al have also shown the potential dissolution of CuO NPs in cell culture medium, but toxicity in A549 lung epithelial cells was only partly dependent on the released of Cu ions. The authors could show a potentially much higher cytotoxicity of CuO NPs than the corresponding ions ($CuCl_2$) (Karlsson, 2008). Another work focussing on Cu release and toxicity has shown that sonication increases release of Cu ions and that dissolution of CuO NPs correlated with the degree of DNA damage in A549 lung epithelial cells, with higher release and toxicity for nanometer-sized particles compared to the micrometer-sized particles (Midander, 2009). Nevertheless, by exposing cells to CuO NPs or the released copper fraction, the authors found that the cytotoxic effects

were mostly caused by the particles and to a lesser extent by the released copper fraction. Based on this findings, it is possible that effects of CuO NPs on cell viability and placental transcriptome could be mediated by CuO NPs rather than the dissolved Cu but further studies would be needed to understand the contribution of particulate versus ionic Cu. Adverse effects were also observed in other cell types (e.g., immune cells, lung cells) after exposure to CuO NPs (Gupta, 2022; Jing, 2015). The CuO NP concentration of 10 μg/mL was chosen for the 6 h *ex vivo* perfusion experiments as it did not result in a significant decrease in BeWo cell viability after a 6 h exposure (SI Figure 2) but is still relatively high to induce transcriptomic changes and to detect potential placental translocation. While there is currently no data available on realistic exposure concentrations for CuO NPs, a recent study identified a mean concentration of 1.6 μg/mL of plastic particles in human blood (Leslie, 2022).

In our earlier publication, 24 h treatment with the same PS NP as the one investigated in the present study did not affect the viability of BeWo cells and placental microvascular endothelial cells at concentrations of up to 100 μg/mL (Aengenheister, 2018). The absence of cytotoxicity after PS administration in placental cells is in line with previous publications, where PS particles did not significantly decrease their mitochondrial activity (Hesler, 2019; Grafmueller, 2015). In addition, in our previous work it was shown that 3 h and 6 h perfusion of human term placenta with similar PS NPs had no influence on placental tissue viability and functionality (Wick, 2010; Grafmueller, 2015). Since higher PS concentrations and longer exposure times did not reveal any signs of cytotoxicity, the concentration of PS NPs to be tested in the transcriptomic profiling was chosen at 25 μg/mL. Although this value is ten-fold higher than systemic concentrations of microplastics detected in blood (1.6 μg/mL) (Leslie, 2022), blood levels for the nanosized fraction of plastic particles in blood are still unknown. With further advances in analytical detection of nanoplastics in complex matrices, we will hopefully better understand whether the chosen concentration is within a realistic range.

Furthermore, we investigated the translocation of CuO NP across the placenta by measuring Cu concentrations in maternal and fetal perfusates (SI Figure 3A). We observed a decrease in maternal Cu levels and a slight increase in fetal Cu concentrations indicating a possible maternal to fetal transfer of CuO NPs or Cu ions. Moreover, Cu concentrations in the placental tissue increased from 4.73 ± 0.87 μg/mL (0 h) to 56.81 ± 30.19 μg/mL after 6 h of perfusion with 10 μg/mL CuO NP suggesting uptake of CuO NPs in placental tissue. A confounding effect from possible Cu contamination in the perfusion medium or from the perfusion setup could be excluded as evidenced from closed maternal perfusion with the medium only in the absence of placental tissue (SI Figure 3B). However, since Cu is naturally present in the placental tissue and ICP-MS can only measure total Cu levels (endogenous and from the added CuO NPs), we performed additional perfusion experiments with plain perfusion medium to understand the extent of endogenous Cu release from the placenta to the maternal and fetal perfusates. This revealed that endogenous Cu was released to both, the maternal and fetal circulation and that Cu levels were similar to those detected in the fetal perfusate from perfusion with CuO NPs. Therefore, we assume that CuO NP transfer to the fetal circulation was probably low in the 6 h of perfusion. A previous study in pregnant mice also observed no translocation of Cu into the placenta or translocation to the fetus by ICP-MS (Adamcakova-Dodd, 2015) whereas oral exposure to Cu microplastics and Cu ions but not to Cu NPs in pregnant rats increased Cu concentration in the fetus (Luo, 2020). However, since exposure in the latter study started already in early pregnancy (GD3), Cu could have distributed in the uterus and surroundings and could therefore be present in the fetus even if Cu did not pass the placenta.

Finally, we also observed that CuO NPs could non-specifically adhere to the perfusion system as verified in closed maternal perfusions with CuO NPs (SI Figure 3B). However, this effect was less pronounced in the *ex vivo* placental perfusion experiments since Cu levels only slightly decreased in maternal perfusates possibly due to the stabilizing effect of proteins released from the tissue covering the particles. Translocation of these 70 PS NPs has been determined in our previous study showing a slow and limited particle crossing after 6 h of placental perfusion (5.5 ± 0.3% of the applied dose) (Furer, 2022). This was lower than translocation reported from previous studies using similar-sized PS NPs (30% of 80 nm PS NPs (25 μg/mL) after 3 h perfusion (Wick, 2010); 11% of 80 nm PS NPs (40 μg/mL) after 6 h perfusion (Gruber, 2020), but could reflect the use of different commercial sources or batches with distinct physico-chemical properties or differences in the perfusion system and protocols (e.g. perfusion medium, albumin content and type, exposure concentrations, flow rates, tubing length, etc.).

3.3. *CuO and PS NPs elicit material-specific and reproducible responses in perfused human placenta*

To understand material specific changes in gene expression, transcriptomic profiling has been used as an effective approach for the simultaneous analysis of all changes in gene expression levels of cells or tissues following NM exposure (Labib, 2016; Kinaret, 2017). Therefore, a whole genome expression analysis by DNA microarrays was performed to identify and compare the effects of CuO and PS NP administration in a perfused human *ex vivo* placental tissue model (NCBI GEO accession number GSE220756). Both CuO and PS NPs caused consistent and

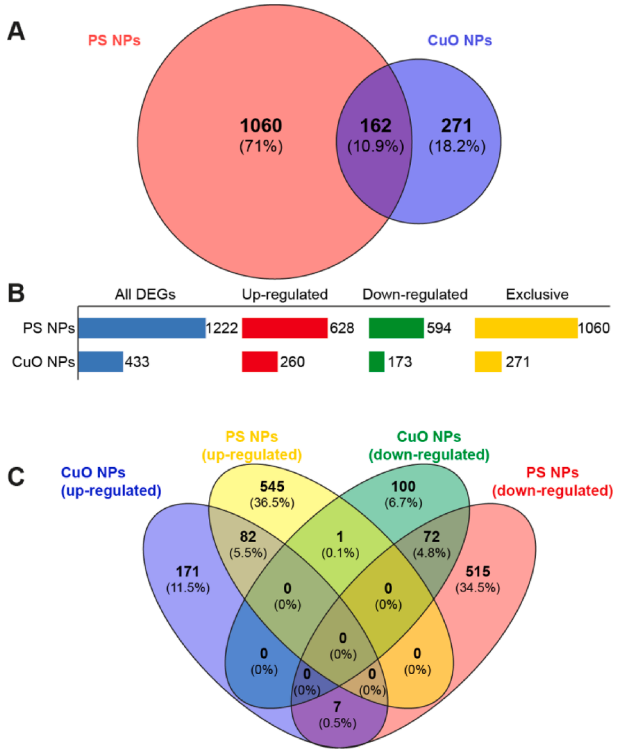

Fig. 1. Impact of CuO and PS NPs on gene expression in perfused human term placenta. **A.** Venn diagram reporting the number of transcripts modulated in response to CuO and PS NP administration in the placenta tissue (cut off level of absolute logFC ≥ 1 and $p \leq 0.01$ were applied). **B.** DEGs with bars representing the number of up- (red) and down- (green) regulated expressed genes. Genes exclusively altered by each treatment are represented with a yellow bar. **C.** Venn diagram demonstrating unique and overlapping differentially up- and down-regulated genes in placenta tissue after CuO and PS NP perfusion for 6 h. Venn diagram depicts the overlap of DEGs from each comparison. The % of modulated genes in each area is reported between the parentheses. Data are from three independent experiments for CuO and PS NP perfusions and two independent experiments for control perfusions with medium only. (For interpretation of the references to color in this figure legend, the reader is referred to the web version of this article.)

robust changes in the gene expression patterns of the perfused placentas as compared to the control tissues (Fig. 1A). However, the numbers of differentially expressed genes (DEGs) showed that CuO NP treatment triggered notably less changes than PS NPs (Fig. 1A). More specifically, a total of 433 genes were significantly differentially expressed (absolute logFC > 1, p value ≤ 0.01) in CuO NP-exposed placentas as compared to controls, while PS NP treatment altered approximately 3-fold more genes (1222 DEGs) (Fig. 1B). 162 (10.9%) of DEGs were common for CuO- and PS NP-exposed groups (Fig. 1B). Among the overlapping genes, 82 DEGs were up-regulated (5.5%) and 80 were down-regulated (5.4%) (Fig. 1C). 171 (11.5%) of the up-regulated DEGs were specific for the CuO NP group and 515 (34.5%) DEGs were specific for the PS NP-treated groups (Fig. 1B-C). Similarly, 100 of DEGs (6.7%) were down-regulated exclusively in CuO NP perfused placentas, and 515 (34.5%) DEGs were down-regulated only in the PS NP group.

The DEGs distribution by magnitude fold-change and significance is shown in the volcano plot with significant DEGs highlighted in red (Fig. 2A). A wide dispersion of the genes was observed indicating a high level of difference in gene expression between the two treatment groups.

To visualize the association between the samples (CuO- and PS-NP treated) a principal component analysis (PCA) was performed (Fig. 2B). The CuO and the PS sample groups were discrete in the PCA and clearly separated. In addition, the negative control group (tissue from perfusion with plain PM only) had also no regions of overlap. Particularly, the PS NP group (left side) and the control group-before perfusion (right side) showed the most visible distinct separation, while the samples from the CuO NP and the control group (after perfusion) being much closer. The pre-perfusion placentas group nicely showing little variation between the samples in the first two principal components. Since all placental samples for microarray analysis were from female fetuses, no sex-specific variability was anticipated. However, further studies including male placenta groups would be needed to elucidate potential sex-specific effects in transcriptome responses to NPs.

3.4. CuO NPs affect expression of genes related to angiogenesis, stress responses and protein misfolding

To gain insights into the biological roles of the over-expressed DEGs after the NM treatments in human placentas we conducted gene ontology (GO) enrichment analysis. Fig. 3A shows the significant over-represented biological processes by the up-regulated DEGs following CuO NP exposure. The top five highly enriched GO terms were angiogenesis (GO:0001525), positive regulation of nitric oxide (NO) biosynthesis (GO:0045429), extracellular matrix organization (GO:0030198), positive regulation of gene expression (GO: 0010628), and muscle contraction (GO:0006936) (SI Table 3). As shown in Fig. 3A the semantically similar enriched GO terms were grouped together forming a bigger GO category. 'Angiogenesis' was the most significant GO category and included biological processes such as positive and negative regulation of angiogenesis, cell differentiation, endothelial development, and morphogenesis, vasculogenesis and bone mineralization, all of which are crucial for proper fetoplacental angiogenic and vascular development and hence influence fetal growth throughout gestation.

A pivotal over-represented GO category indirectly related to angiogenesis was the 'positive regulation of nitric oxide biosynthesis'. NO produced by endothelial cells and inducible NO synthases act in multiple pathways participating in implantation, angiogenesis and vascular development and are actively involved in embryonic development (Krause et al., 2011). Higher NO production has been associated with human pregnancy complications such as intrauterine growth restriction (IUGR), fetal hypoxia and preeclampsia (Abán, 2018; Tikvica, 2008; Jurado, 2019).

The enriched GO terms in the GO cluster 'response to heat' were consistently associated with responses to hormone and transforming growth factor beta stimulus, regulation of inflammatory and oxidative stress responses, and responses to unfolded proteins. *FOS*, *JUND*, *PGF* and *RAMP3* genes were enriched in the term 'response to hormone stimulus' (GO: 0032870, top 10 of GO terms). Among those genes, *FOS* has been shown to control the regulation of trophoblast migration and invasion which is essential for sufficient maternal blood supply and placental development (Renaud, 2014; Wang, 2020). De-regulation of *FOS* gene has been associated with placental-related pregnancy complications *i.e.,* preeclampsia and abortion and has a negative impact on the neurobehavioural development of the offspring (Wang, 2020; Mackenzie, 2012; Marzioni, 2010; Zheng, 2018). In addition, over-expression of *JUND* gene impairs placental vascularization and embryonic growth (Kashif, 2012). Oxidative stress (due to reactive oxygen species formation *via* interaction with biomolecules or particle surface interactions) (Angelé-Martínez, 2017) and pronounced inflammatory responses are the commonly observed adverse effects after CuO NP exposure in both cellular and animal studies (Strauch, 2017; Lai, 2018; Cho, 2012).

The observed enriched processes related to unfolded proteins response, protein folding, and ubiquitination was caused by the upregulation of several heat shock protein (HSP) transcripts, namely *HSPA1a* (logFC:1.3), *HSPA1b* (logFC: 1.9), *HSPA6* (logFC: 2.2), *HSP90AA1*(logFC:1.6) and *HSP90AA2P* (logFC:1.1) which are responsible for proper protein folding, degradation of un- or misfolded proteins and are increased in response to cellular stress (Daugaard et al., 2007). Saporito-Magrina *et al.*, demonstrated that cells initiate heat shock responses after Cu treatment as a protective mechanism to restore protein homeostasis, resulting ultimately in cell death (Saporito-Magriñá, 2018). Similar responses related to upregulated heat shock proteins

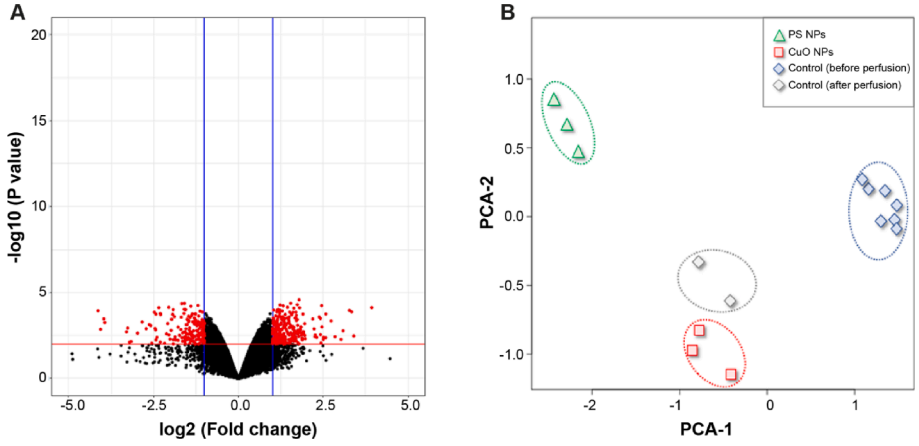

Fig. 2. Volcano plot and principal component analysis (PCA) A. Volcano plot displaying gene expression changes in human *ex vivo* placentas perfused with CuO or PS NPs for 6 h. The significant deregulated genes are reported in red ($p \leq 0.01$). The black points represent genes with a p-value higher than 0.01. The blue vertical margins represent the logFC cut off. The red horizontal margin depicts the p value cut off. **B.** PCA plots showing the relationship between the samples (CuO-treated, PS-treated, control-before perfusion, control-after perfusion). Colored oval shapes with dashed lines depict the different sample groups for better visualization. Volcano plot and PCA analysis has been performed with eUTOPIA platform. Group size is n = 3 for CuO and PS NPs; n = 2 for controls (after perfusion) and n = 8 for controls (before perfusion). (For interpretation of the references to color in this figure legend, the reader is referred to the web version of this article.)

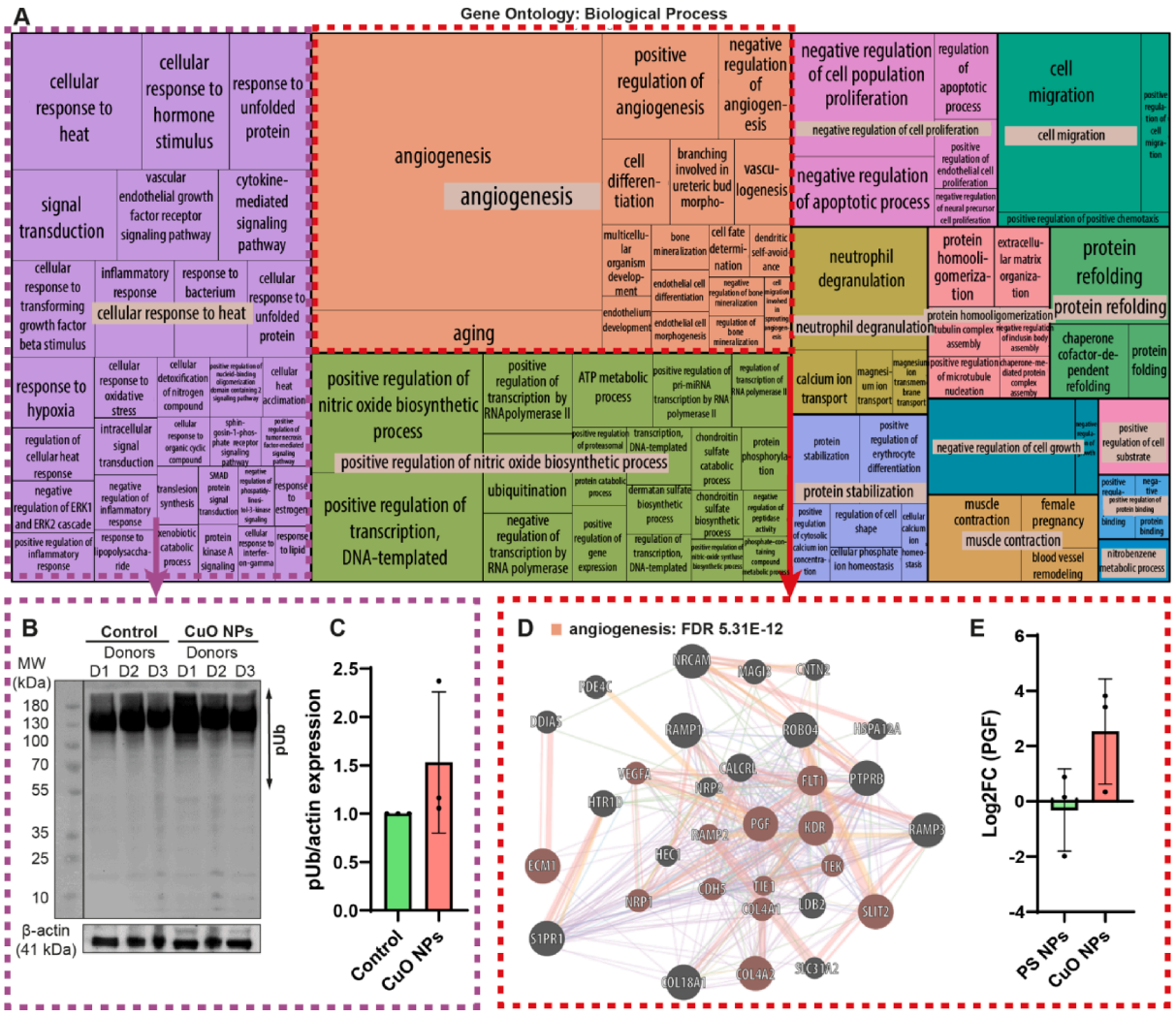

Fig. 3. Gene Ontology (GO) enrichment analysis after CuO NP treatment. **A.** Upregulated highly enriched biological processes following CuO NP treatment are summarized in the tile plot. Each rectangle represents a single GO term, contained in a bigger rectangle in which semantically similar GO terms are grouped together. The size of the rectangles reflects the *p* value. Treemap was obtained with INfORM platform. (Full page figure available in SI Figure S4). **B.** Immunoblot shows an increased accumulation of polyubiquitinated (pUb) proteins in the placental tissue after exposure to CuO NPs indicating protein misfolding. **C.** Relative quantification of pUB expression with respect to beta-actin (loading control). **D.** Angiogenesis, attributed to a subset of 11 genes, was identified as the most highly enriched (*p* value: 1.73×10^{-11}) biological process within the upregulated DEGs from CuO NP exposure. The connections between gene nodes represent physical, predicted, and genetic interactions as well as shared protein domains and pathways. Gene interactions were visualized using the GENEmania online tool. **E.** Expression of *PGF* gene in placentas perfused with CuO NPs or PS NPs with respect to control. Data (C, E) presented as a mean ± standard deviation (n = 3 donors). Group size in A, D is n = 3 for CuO and PS NPs and n = 2 for controls.

were reported following a transcriptomic and proteomic-based analysis in CuO NP-exposed lung epithelial cells and THP-1 macrophages respectively, indicating a potential signature response for CuO NP administration (Boyadzhiev, 2021; Tarasova, 2017).

In a recently discovered mechanism of copper-mediated cell death (termed cuproptosis), misfolding of mitochondrial or cytosolic proteins has been demonstrated to play an essential role in cell death (Gupta, 2022; Tsvetkov, 2022). Using a copper ionophore (elesclomol), Tsvetkov *et al.* could show that an increased copper load in the cells triggered aggregation of lipoylated proteins in mitochondria, which then led to proteotoxic stress and ultimately cell death (Tsvetkov, 2022). In another study using a RAW macrophage cell line, Gupta *et al.* could show that intracellular dissolution of CuO NPs in lysosomes triggered misfolding of cytosolic Cu/Zn SOD1 and proteasomal dysfunction, which eventually led to the macrophage cell death by proteostatic stress (Gupta, 2022). A marked differential expression of multiple genes or integrated pathways related to unfolded proteins response or heat-shock responses in the present study could be an indication of copper-mediated proteotoxicity because of the accumulation of misfolded protein aggregates. Therefore, we validated protein misfolding in placental tissue by detecting the accumulation of polyubiquitinated proteins by immunoblotting. As expected, an increased accumulation of polyubiquitinated proteins was observed in placental tissues exposed to CuO NPs as compared to the control (Fig. 3B-C). Hence, the results confirmed that the heat-shock response observed in the microarray data corresponds to the stress response from the accumulation of misfolded protein. The accumulation of misfolded proteins or pathological protein aggregates in maternal tissue is a well-established mechanism of preeclampsia in pregnancy (Redman and Sargent, 2005; Buhimschi, 2014). Therefore, our results may have direct implications for preeclampsia in pregnancy. However, the dose of CuO NPs used in the present study is likely higher than the one individuals are currently exposed to under realistic conditions. Nonetheless, the risk cannot be neglected and our study recommends a further detailed investigation of such effects of CuO NPs at long-term exposure using a realistic dose.

Furthermore, focusing on angiogenesis (GO:0001525; FDR: 5.31 ×

10^{12}; *p*: 1.73 × 10^{11}) the highest enriched biological pathway was enriched by eleven DEGs, including a subset of up-regulated extracellular matrix related genes including *COL18A1* (logFC:1.6), *COL4A2* (logFC:1.4), and *ECM1* (logFC:2) and *KDR* (logFC:1.7), the main receptor for vascular endothelial growth factor (VEGF) in endothelial cells (Fig. 3D). KDR kinase is long known to function as a promoter of VEGF-induced endothelial cell proliferation, survival, differentiation and tubular morphogenesis (Tao, 2001). Furthermore, it is essential for the regulation of angiogenesis, vascular development and permeability, as well as in embryonic hematopoiesis (Tao, 2001). Increased *KDR* expression has been found in hypoxic/ischemic regions of villous blood vessels in human placentas under pathological conditions (Kumazaki, 2002). The observed upregulation of *KDR* may be also linked with the positive regulation of NO production, as KDR is involved in the VEGFA-mediated induction of NOS2 and NOS3, leading to the endothelial production of NO (Duval, 2003).

A key molecular player in angiogenesis is placenta growth factor protein (PGF), which was highly enriched after placental CuO NP exposure (logFC: 1.3). *PGF* has a central role in the interaction gene network of angiogenesis (GO:0001525) (Fig. 3D) and was associated with significant enrichment of similar biological processes, such as response to hormone stimulus (GO:0032870), vascular endothelial growth factor receptor signaling (GO:0048010), female pregnancy (GO:0007565) and regulation of endothelial cell proliferation (GO:00001938). Similar to KDR, PGF belongs also to the VEGF protein family with a primary role to induce pro-angiogenic effects on the feto-placental circulation and to support trophoblast growth and differentiation (De Falco, 2012). Several studies demonstrated elevated levels of *PGF* at hypoxic conditions, but the molecular basis of hypoxia-induced *PGF* expression has not been yet clarified (Tudisco, 2017; Thompson, 2016). Importantly, long-lasting placental hypoxia can provoke placental insufficiencies caused by abnormalities in trophoblast development and remodeling of maternal spiral arteries and could potentially lead to PE and maternal hypertension (Thompson, 2016). Comparable to *KDR*; *PGF* has also a functional link with endothelial nitric oxide synthase (*eNOS*) playing a vital role in the regulation of pathological angiogenesis (Gigante, 2006). Gene expression levels of *PGF* were validated in a new set of perfusion experiments (three donors not used for microarray analysis) by qPCR and confirmed an elevated (logFC: 0.78) expression of *PGF* in CuO NP-exposed placenta (Fig. 3E). The observed high deviations across the independent replicates is inevitably induced by the use of placentas derived from different donors. However, such donor-dependent variation is often observed in *ex vivo* experiments and *in vitro* experiments with primary cells and is reflecting the heterogeneity in the human population, indicating a real-world situation (Song et al., 2011; Chortarea, 2017; Mohammadi, 2021). Moreover, by using genomic-based approaches the cellular and molecular mechanisms underlying the donor-to-donor variability can be determined. In addition to donor variations, another factor that could potentially account for the high deviations in the data could be sex-specific differences for placentas derived from male or female fetuses. Sex differences on placental transcriptome have been shown for placentas from term pregnancies (Sood, 2006; Buckberry, 2014; Sedlmeier, 2014) and more recently also for early pregnancy (reviewed in (Braun, 2022) and revealed widespread differences in endocrine signaling, immune signaling and metabolic functions, which may contribute to altered growth and developmental outcomes for the fetus (Meakin, 2021). On the other hand, two recent studies did not find an associations between placental sex and the biodistribution and/or fetoplacental effects of NPs (TiO_2 or carbon black) (D'Errico, 2022; Bongaerts, 2022). In our study, qPCR samples were from mixed sexes for the PS NP group (2 females/1 male) but from same sex within control (3 males) and CuO NP groups (3 females). Although our study was not designed to investigate sex-specific responses, we briefly discussed the results in relation to placental sex of the samples. For all experiments with CuO NP perfused groups, we can exclude that data variability is related to placental sex (all female placentas) but conclusions on sex-specific effects are not possible (no males in CuO group; no females in control group). For PS NP group, *PGF* was slightly upregulated only for the male sample whereas the two female samples showed no or moderately reduced expression. However, larger study groups would be needed to understand if this reflects a potential sex-specific response to PS NP exposure.

Kyoto Encyclopedia of Genes and Genomes (KEGG) pathway analysis after CuO NP exposure revealed that the DEGs highly enriched three hormone-related pathways: 'Estrogen signaling pathway', 'Ovarian steroidogenesis' and 'Parathyroid hormone synthesis, secretion and action' (Table 1). Hormones influence various aspects of placental function and fetal development, particularly the vascularization, fetal follicular maturation, development of the ovaries and the nervous system and play a crucial role in pregnancy maintenance (Albrecht and Pepe, 2010; Berkane, 2017; Chan et al., 2009). More specifically, estrogens are essential for vasodilation and local angiogenesis due to their interaction with VEGF and PGF (Dugershaw, 2020; Berkane, 2017). In addition, based on the ranking of the top 15 pathways, three pathways related to nutrient and xenobiotic metabolism were over-represented *i.e.*, 'Protein digestion and absorption', 'Riboflavin metabolism' and 'Metabolism of xenobiotics by cytochrome P450′. Perturbations in metabolic and nutrient signaling pathways have been identified in pregnancy disorders such as IUGR, gestational diabetes, and maternal obesity (Paquette, 2018). Moreover, pathways associated with signal transduction were also significantly enriched ('Antigen processing and presentation', 'Cytokine-cytokine receptor interaction' and 'MARK signaling pathway',

Table 1
Summary of the top fifteen significantly enriched KEGG pathways in human *ex vivo* placentas following CuO NP exposure (at concentration of 10 μg/mL).

KEGG Pathway Term	P-Value	No. Genes	Gene Names
Estrogen signaling pathway	1.98E-04	11	POMC;HSP90AA1;KRT19; KRT27;HSPA6;KRT14;ITPR1; ADCY4;FOS;HSPA1B;HSPA1A
Protein digestion and absorption	7.45E-04	8	COL18A1;MME;COL4A2; COL14A1;COL5A3;COL7A1; SLC1A1;COL4A5
Rheumatoid arthritis	0.003609	7	FLT1;TGFB3;ITGB2;ACP5;FOS; TEK; TNFSF13B
Ovarian steroidogenesis	0.004051	5	HSD17B1;LHB;ADCY4;CGA; BMP6
Fluid shear stress and atherosclerosis	0.01201	8	CDH5;GSTM3;HSP90AA1; GSTM1;GSTO1;CAV1;KDR; FOS
Riboflavin metabolism	0.018397	2	ENPP1;ACP5
Cell cycle	0.018397	7	CCNB2;PTTG1;PTTG2;TGFB3; SFN; TTK;MAD2L1
Metabolism of xenobiotics by cytochrome P450	0.022122	5	CBR1;ALDH1A3;GSTM3; GSTM1;GSTO1
Pathways in cancer	0.022705	19	GSTM3;HSP90AA1;GSTM1; DAPK1;GSTO1;TGFB3; NOTCH4;LAMA4;ADCY4;FOS; GNG11;PGF;BMP2;COL4A2; TRAF3;IL3RA;COL4A5;BIRC7; JAK2
Longevity regulation pathway	0.023519	6	KL;HSPA6;ADCY4;CRYAB; HSPA1B;HSPA1A
Vascular smooth muscle contraction	0.024926	7	NPPB;ACTA2;RAMP3;ITPR1; ADCY4;MYL9;ACTG2
Antigen processing and presentation	0.02576	5	HSP90AA1;HSPA6;KLRD1; HSPA1B;HSPA1A
Cytokine-cytokine receptor interaction	0.027145	12	ACVRL1;NGFR;IL33;BMP2; TGFB3;LEP;IL24;IL3RA;INHA; IL18R1;BMP6;TNFSF13B
Parathyroid hormone synthesis,secretion and action	0.027759	6	SLC9A3R1;KL;JUND;ITPR1; ADCY4;FOS
MAPK signaling pathway	0.027766	12	DUSP4;NGFR;JUND;FLT1; TGB3;HSPA6;KDR;FOS;TEK; HSPA1B;PGF;HSPA1A

Table 1) as a result of CuO NP exposure.

3.5. PS NPs affect expression of genes related to inflammation and iron homeostasis

Analysis of the top 10 most enriched GO underlying PS NP responses in human *ex vivo* placentas pointed out several GO terms related to cell division and cell cycle: translesion synthesis (GO:0019985), DNA repair (GO:0006281), regulation of G2/M transition of mitotic cell cycle (GO:0010389), regulation of signaling receptor activity (GO:0010469), error-prone translesion synthesis (GO:0042276) and G2/M transition of mitotic cell cycle (GO:0000086). Two GO terms (apoptosis (GO:0006915) and negative regulation of apoptotic process (GO:0043066)) were associated with apoptosis. In addition, two of the most represented GO-term was inflammatory response (GO:0006954) and response to lipopolysaccharide (GO:0032496) (SI Table 4).

As shown in Fig. 4A, 'inflammatory response' is also a significantly over-represented GO group, consisting of biological responses like responses to cytokines and chemokines, hormones (estradiol, progesterone), minerals, hypoxia, or stress-related responses (heat). Immune-related responses were also induced by placental PS NP administration, including the GO categories of 'neutrophil degranulation', 'response to LPS' and 'chemotaxis'.

Placental exposure to engineered NMs, such as titanium dioxide (TiO_2) and Ag NPs, has been associated with dysregulation of placental vascularization, proliferation and apoptosis (Zhang, 2018). In addition, multi-walled carbon nanotubes (MWCNTs) resulted in p53-dependent apoptosis and cell cycle arrest in response to DNA damage in placental tissue of exposed pregnant mice (Huang, 2014). In the present study, placental PS NP exposure also demonstrated high enrichment of GO categories related to 'regulation of G2/M transition in cell cycle', 'cell division', 'negative regulation of cell growth', 'cell proliferation' but also 'apoptosis' (Fig. 4A).

Inflammatory response (top 10 most enriched GO terms, GO:0006954, *p*: 4.02754 x10^{9}) was enriched by 21 genes, including cytokine/chemokine genes (*IL-6*, *CCL17*, *CCL2*, *CCL7*, *IL36G*, *CXCR4*, *LTBR*), transforming growth factor-β (TGF-β) related / induced genes (*BMP2*, *CDO1*), histamine-related genes (*HRH1*, *HDAC9*), extracellular

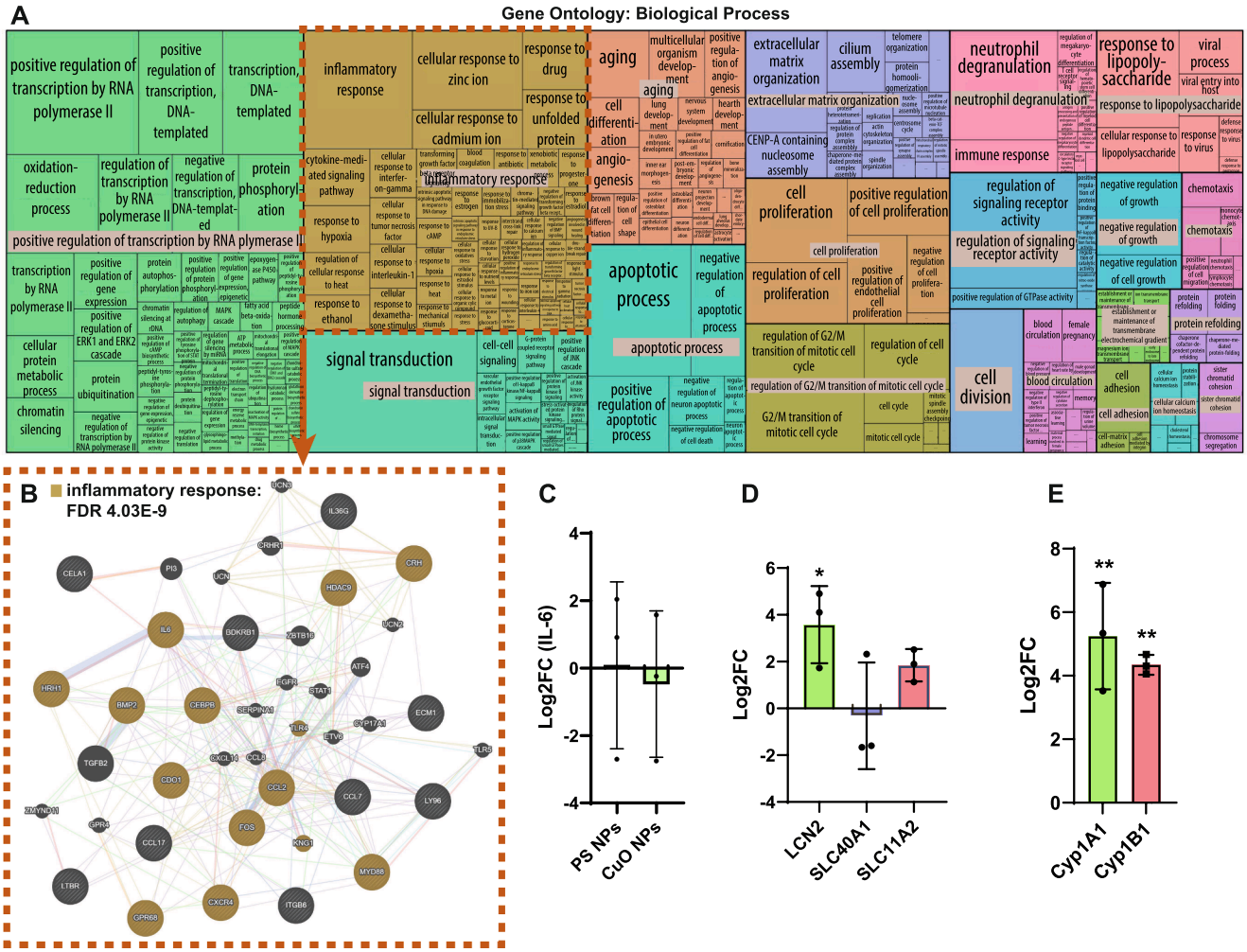

Fig. 4. Gene Ontology enrichment analysis after PS NP treatment. **A.** The tree-map summarizes highly enriched biological processes following PS NP treatment. Each rectangle represents a single GO term, contained in a bigger rectangle in which semantically similar GO terms are grouped together. The size of the rectangles reflects the *p* value. Treemap was obtained with INfORM platform. (Full page figure available in SI Figure S5). **B.** Inflammatory responses, attributed to a subset of 12 genes, was identified as the most highly enriched (*p* value: 4.03 × 10^{-9}) biological process within the de-regulated DEGs of PS NP exposure. The connections between gene nodes represent physical, predicted, and genetic interactions as well as shared protein domains and pathways. 'Gene interactions were visualized using the GENEmania online tool. **C.** Gene expression of *IL-6* gene in PS or CuO NP-treated *ex vivo* placentas. **D.** PS NPs effects on iron homeostasis in placental tissue at mRNA level (iron binding protein LCN2 and iron transporters SLC40A1 and SLC11A2). **E.** Change in the mRNA expression of cytochrome P450 isoenzymes after exposure to PS NPs. Data in C-E represent mean ± standard deviation (n = 3). * $p < 0.05$, ** $p < 0.01$ vs. neg. control. Group size in A, B is n = 3 for CuO and PS NPs and n = 2 for controls.

matrix and adhesion genes (*ITGB6*, *ECM1*), immune response related genes (MYD88, LH96), receptors (*BDKRB1*, *GPR68*), and hormone gene (*CRH*).

Among the cytokines, *IL-6* gene is highly interacting with other genes in the inflammation GO gene network (Fig. 4B) and appeared in several additional GOs enriched by PS NPs (e.g., cytokine-mediated signaling pathway (GO:0019221), positive regulation of cell proliferation (GO:0008284), positive regulation of gene expression (GO:0010628), monocyte chemotaxis (GO:0002548), response to heat (GO:0009408) and cellular response to nutrient levels (GO:0031669)). IL-6 release is pivotal in inflammation (acute and chronic) and autoimmunity, as it is involved in leukocyte recruitment, activation, differentiation, and apoptosis (Gabay, 2006; Naugler and Karin, 2008). Notably, there is compelling evidence, indicating that elevated levels of IL-6 are implicated in unexplained infertility, recurrent miscarriages, preeclampsia and pre-term delivery, due to its modulating role in blastocyst implantation and placental development (Wu, 2017; Prins et al., 2012). Metal oxide- and carbon-based NMs have been reported to induce the release of IL-6 in various cell types and tissues (including placenta), leading to pro-inflammatory responses (Chortarea, 2017; Shirasuna, 2015; Paul, 2017; Colombo, 2019). More recently IL-6 has been identified to be highly deregulated in response to PS NPs in a size-dependent and concentration-dependent manner in immune cells (Prietl, 2014; Hwang, 2020). Therefore, we further investigated the expression levels of *IL-6* in placental tissues by qPCR, demonstrating a weak upregulation of *IL-6* after PS exposure due to high donor variability (pronounced upregulation in 2 donors and down-regulation in one donor), and a slight *IL-6* down-regulation following CuO NP administration (Fig. 5C). Interestingly, a recent study in pregnant mice observed sex-specific inflammatory responses in LPS-exposed mice including higher levels of IL-6 in male placentas than female placentas (Braun, 2019). In this study, *IL-6* was upregulated in the two female samples, while it was downregulated in the male sample, which could indicate a potential higher pro-inflammatory response to PS NPs in female placentas. However, additional studies with larger group sizes for both sexes are warranted to draw firm conclusions on potential sex-specific responses.

To further understand and validate the downstream effects of IL-6 upregulation, we performed qPCR analysis of three differentially expressed genes in microarray experiments, namely *LCN2* (Lipocalin 2), *SLC40A1* (Solute Carrier Family 40 Member 1 or Ferroportin 1) and *SLC11A2* (Solute Carrier Family 11 Member 2 or Proton-Coupled Divalent Metal Ion Transporter 1 (DMT 1)). The qPCR results demonstrated an increased expression of *LCN2*, and *SLC11A2* genes in PS NPs exposed placental tissue with respect to the negative control (untreated), while transcription levels of *SLC40A1* were maintained (Fig. 4D). Highest upregulation of *LCN2*, *SLC11A2* and *SLC40A1* was observed for the male sample. Previous studies have shown that bacterial infections or LPS exposure can upregulate the expression of proinflammatory cytokines (e.g., IL-6) in mammalian cells and mice, which in turn leads to a cascade of events to counteract inflammation by lowering the cellular iron level, for example, via upregulation of iron-chelating protein LCN2 (Borkham-Kamphorst, 2013; Hop, 2018; Nairz, 2015; Cassat and Skaar, 2013). Furthermore, in a feedback mechanism to the low cellular iron level in the placenta, a maintained or even slightly reduced mRNA expression of the iron exporter (*SLC40A1*) and increased expression of the iron importer (*SLC11A2*) was observed to keep the iron homeostasis (Fig. 4E). SLC11A2 and SLC40A1 (Ferroportin 1) have been shown to play an important regulatory function in the iron homeostasis of maternal and intestinal cells in rats (Sangkhae, 2020; Cornock, 2013; Gunshin, 2005). Authors could demonstrate that supplementing a low iron diet to rats changed the expression profile of iron-regulating genes including *SLC11A2* (Cornock, 2013).

Cytochrome P450 isoenzymes (Cyps) have known functions in metabolizing and detoxifying pharmaceutical drugs and aryl hydrocarbons in humans (Chang and Kam, 1999). PS NPs have been shown to affect the function of Cytochrome P450 enzymes in a size-dependent manner (Fröhlich, 2010). The authors could show that small (20–60 nm) PS particles but not larger (200 nm) ones inhibited the enzymatic

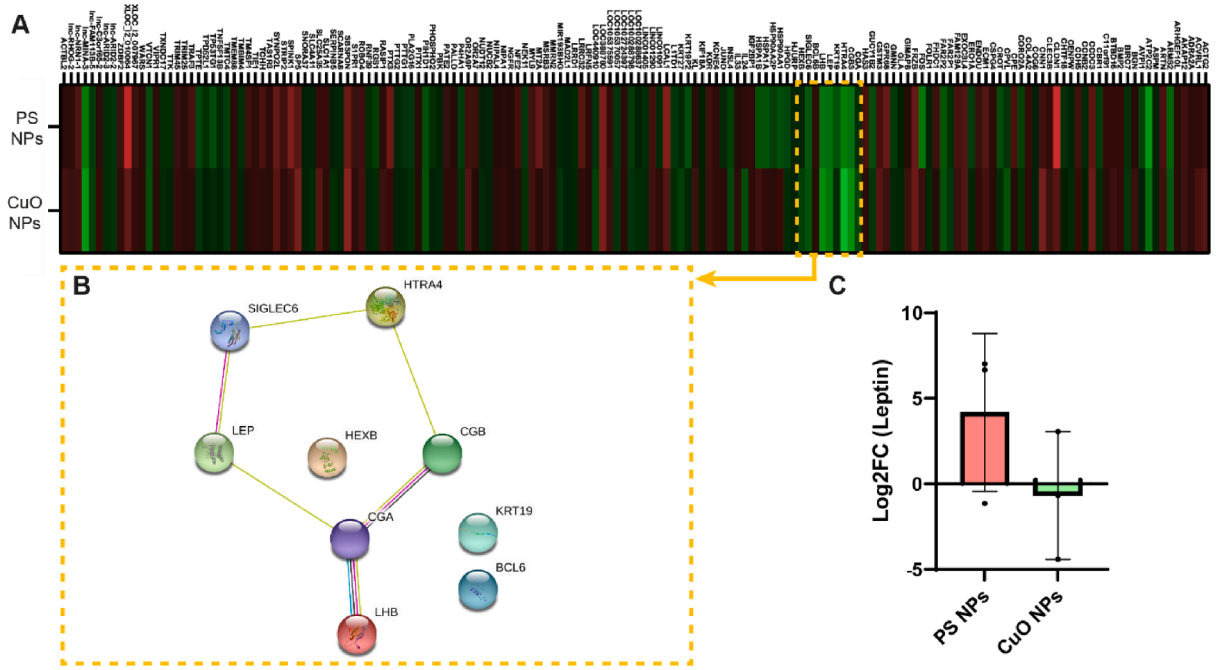

Fig. 5. A. Heatmap of the 162 common DEGs after CuO and PS NP exposures in the human *ex vivo* placenta model. Up-regulated genes are presented in red, while down-regulated genes appear in green. The yellow dashed box highlights the most down-regulated genes in both treatments. **B.** The highlighted genes were subjected to network analysis. The connections (edges) between the gene nodes represent physical, predicted, and genetic interactions. Gene network analysis was performed using the STRING online tool for functional interaction networks. **C.** Gene expression (LogFC) of the selected signature gene *LEPTIN*. Data in C represent mean ± standard deviation (n = 3). Group size in A, B is n = 3 for CuO and PS NPs and n = 2 for controls. (For interpretation of the references to color in this figure legend, the reader is referred to the web version of this article.)

activity of CYP450 isoenzymes (*CYP3A4, CYP2D6, CYP2C9* and *CYP2A1*) in BACULOSOMES® (insect cells engineered to express Cyps isoenzymes) and substrate cleavage in normal liver microsomes. In the present study, we observed an increased expression of Cyps (*Cyp1A1* and *Cyp1B1*) in transcriptomics profiling after exposure to the PS NPs, which was validated by qPCR (Fig. 4E). In this case, the response was more pronounced for the two female samples and was lowest for the male sample. This is opposite to the iron homeostasis genes where the highest expression was induced in the male sample, thus there seems to be no clear trend for one sex being more vulnerable to PS NP exposure. KEGG pathway analysis yielded more detailed information on the molecular pathways, potentially activated in PS NP-perfused placental tissue (Table 2). Similar to CuO NP responses, the over-expressed genes after PS NP administration showed significant enrichment of pathways related to nutrient metabolism and absorption *i.e.,* 'Mineral absorption', 'Folate biosynthesis', 'Amino sugar and nucleotide sugar metabolism' and 'Glycerolipid metabolism'. It is well-known that proper maternal nutrition is essential for the normal growth and development of the fetus (Barua, 2014; Busso et al., 2020; Marshall, 2022). While glucose metabolism is considered the main energetic source, macronutrients (e.g., lipids) that supply structural and energetic functions and micronutrients like vitamins and minerals are major intrauterine environmental factors, necessary for the normal organ development and functioning of metabolic pathways (Díaz et al., 2014; Mousa et al., 2019; Farias, 2020). Folate, also known as vitamin B9, is a vital nutrient important for DNA replication but also for a variety of enzymatic reactions related to amino acid synthesis and vitamin metabolism (Greenberg, 2011). Nutritional deficits of these different nutrient classes may potentially modulate susceptibility to various maternal and fetal diseases. In agreement with our observations on the enrichment of nutrient metabolism and transport related pathways after PS NP exposure, Mahler *et al.*, demonstrated that acute and chronic oral exposure to PS NPs could interfere with mineral absorption and transport (Mahler, 2012). Moreover, in a recent *in vitro* study ZnO NPs altered nutrient uptake and transport in a small intestinal cell model (Moreno-Olivas et al., 2019).

Table 2
Summary of the top fifteen significantly enriched KEGG pathways in human *ex vivo* placentas following PS NP exposure (at concentration of 25 μg/mL).

KEGG Pathway Term	P-Value	No. Genes	Gene Names
Mineral absorption	2.24E-07	15	SLC34A2;MT1M;SLC11A2; SLC40A1;ATPP1A4;MT1X; ATP1B1;MT2A;MT1A;MT1F; MT1G;MT1H;MT1B;MT1HL1; MT1E
IL-17 signaling pathway	2.83E-06	19	CSF3;HSP90AA1;CEBPB;JUND; TRAF3IP2;FOS;IL17RB;RELA; NFKB1;FOSL1;IL6;CCL7;TRAF3; LCN2;CCL2;DEFB4A;MAPK6; IKBKE;CCL17
NF-kappa B signaling pathway	1.94E-04	16	GADD45B;IL1R1;LY96;TRAF1; CFLAR;TICAM1;RELANFKB1; TNFSF13B;NFKB2;PLAU;TRAF3; TRIM25;LTBR;CARD14;MYD88
Fanconi anemia pathway	0.001422	10	FANCI;RAD51C;FANCM;FANCL; UBE2T;RPA3;PLI;BRACA1;PLK; FANCE
Legionellosis	0.001645	10	HSPA8;VCP;IL6;BNIP3;RELA; NFKB1;HSPA1B;MYD88;NFKB2; HSPA1A
Cell cycle	0.003647	16	PCNA;CDKN2C;GADD45B; BUB1B;TTK;CDC25B;GADD45G; CCNB2;WEE1;PTTG1;TFDP2; PTTG2;CCNE1;ORC3;MCM6; MAD2L1
Small cell lung cancer	0.004215	13	LAMB3;GADD45B;ITGA3; TRAF1;RELA;NFKB1;GADD45G; COL4A2;TRAF3;CCNE1;CKS2; POLK;BIRC7
Fluid shear stress and atherosclerosis	0.004849	17	GSTM3;HSP90AA1;BMPR2; SDC4;IL1R1;DUSP1;MGST3; ITGB3;KEAP1;MGST2;FOS; NFKB1;RELA;CDH5;KDR;CCL2; SQSTM1
DNA replication	0.005468	7	RFC5;RNASEH2C;PCNA;RFC4; PRIM1;RPA3;MCM6
Mismatch repair	0.011285	5	RFC5,PCNA;RFC4;MSH2;RPA3
Proximal tubule bicarbonate reclamation	0.011285	5	MDH1;ATP1A4;ATP1B1;GLS; PCK2
Human T-cell leukemia virus 1 infection	0.015123	23	STAT5A;CDKN2C;IL1R1;NFYB; BUB1B;FOS;RELA;NFKB1; NFKB2;FOSL1;POLB;CCNB2;IL6; XPO1;HLADMB;PTTG1;PTTG2; CCNE1;VDAC3;LTBR;ATF4; MAD2L1
Folate biosynthesis	0.018966	5	QDPR;CBR1;GCH1;ALPP; AKR1B1
Amino sugar and nucleotide sugar metabolism	0.025633	7	CYB5R1;UGP2;HEXB;FPGT; GFPT2;PGM1;GNE
Glycerolipid metabolism	0.031474	8	ALDH1B1;LIPG;MBOAT1; AKR1B1;GPAT3;ALDH7A1; AGPAT2;GLA

In addition, PS NP exposure significantly enriched KEGG pathways related to immune and inflammatory responses: 'IL-17 signaling pathway', 'NF-kappa Beta signaling pathway', 'Legionellosis' and 'Human T cell Leukemia virus infection' (Table 2). In agreement with the over-represented GOs underlying PS NP responses in *ex vivo* placentas, KEGG pathways associated to cell cycle and cell proliferation were also observed *i.e.,* 'Cell cycle', 'DNA replication' 'Mismatch repair' and 'Fanconi anemia pathway'.

3.6. The most deregulated common genes between CuO and PS NPs include genes associated with hormone metabolic processes

Eleven % of DEGs (162 genes) were common for both NP groups (Fig. 5A). According to the over representation analysis, the highest enriched GO terms were mainly associated with response to growth factor stimulus, transforming growth factor beta receptor signaling pathway (GO:0071560) and cytokine production (GO: 0071560, GO:0007179, GO:0001817), as well as GO related to regulation of endothelial cell proliferation and cell differentiation (GO:0001936, GO:0045446) (SI Table 5). Analysis of the overlapping genes indicated that crucial molecular perturbations at the gene expression and pathway level in the human placenta were consistent after NM exposure, regardless of the class of NMs studied (metal oxide- versus polymer-based NMs). Nevertheless, the magnitude (fold-change response) of the de-regulation varied. A heatmap of the up- and down-regulated overlapping genes is shown on Fig. 5A. The 10 most de-regulated genes are highlighted in the heatmap and are associated with hormone metabolic processes and reproductive system development processes (Fig. 5B). Interestingly, the majority in this gene group included the hormone-related genes *LEP*, *LHB*, *CGA*, *CGB, HTRA4, SIGLEC6* which are implicated specifically in placental function and pregnancy outcome (Napso, 2018). Several studies have shown that molecules generated by these genes might have a role in the pathogenesis of pre-eclampsia and other pregnancy complications and hence are studied as potential biomarkers for the prediction or detection of such aggravations (Sõber, 2015; Kaartokallio, 2015; Rumer, 2013). NM interference with placental endocrine function also has been described in a recent study, revealing that pristine PS NPs induced a down-regulation of the expression of *HSD17B1* (involved in steroid hormone synthesis) in syncytialized BeWo b30 cells (Dusza, 2022).

As shown in Fig. 5B, *LEP* has been identified as a hub gene. Leptin is produced by the syncytiotrophoblast, affecting maternal metabolism, crucial placental functions (e.g. angiogenesis, growth, and immune tolerance) and fetal development (Pérez-Pérez, 2018; Briffa, 2015). Placental leptin de-regulation is suspected in pregnancy pathologies and

is associated with growth defects and metabolic anomalies (de Knegt, 2021; Bick, 1998; Miehle et al., 2012; Chrelias, 2016). To further determine the expression of this signature gene in placental tissue after *ex vivo* perfusion exposure to CuO or PS NPs, qPCR was performed. *LEP* was down-regulated following CuO NP administration, while it was up-regulated after PS NP exposure (Fig. 5C).

A transcriptomic analysis can only provide an indication of potential deregulated protein levels and functions due to consequential translation and post-translational modifications. Nevertheless, it was pointed out that potential placental exposure to engineered NMs might be associated with major physiological and molecular changes which could affect normal fetal development. Whether the observed transcriptomic changes can be reflected to functional protein changes after single or repeated NM maternal exposure and in what extend it might influence healthy and high-risk pregnancies requires further research.

4. Conclusion

Our results demonstrated that maternal exposure to CuO NP and PS nanoplastic in an *ex vivo* human placenta model can elicit material-specific transcriptional changes in the placental tissue. By applying whole genome microarray analysis of perfused placental tissue, we could show that CuO NPs triggered stress responses related to protein misfolding (e.g. cellular response to heat, angiogenesis, and cellular protein homeostasis). The cellular accumulation of misfolded protein was further validated by detecting polyubiquitinated proteins by immunoblotting. These results suggest that exposure to CuO NPs may trigger cuproptosis, a recently discovered cell death mechanism induced by abnormal accumulation of misfolded protein aggregates in the cells (Tsvetkov, 2022). On the other hand, PS NP exposure elicited transcriptional changes related to the dysregulation of inflammatory factors (e.g., IL-6) and iron homeostasis. The expression of genes encoding iron-siderophore (lipocalin-2) and iron exporter (SLC40A1) were increased, which is typically observed as a cellular response to pathogen infection (Hop, 2018; Nairz, 2015).

Overall, the findings of the present study have important implications for the health and safety of pregnant women and demonstrate that the placenta constitutes an essential signaling interface that is prone to NP induced interferences. Currently, the placenta is mostly studied for its barrier function to restrict NP translocation to the fetus. However, systematic studies on the effects of NPs on placental functions essential to embryo-fetal development are scarce and mostly derived from pregnant animals which cannot be directly extrapolated to humans due to considerable species-specific differences. This study unveiled novel human-relevant toxicity mechanisms of CuO and PS NPs at sub-cytotoxic concentrations already from a single short-term exposure. Therefore, future studies are warranted to understand if these changes persist and adversely affect embryo-fetal development. Moreover, it would be important to verify if similar changes would be induced by CuO and PS NPs in early gestation with the highest susceptibility of the developing fetus. While *ex vivo* placenta perfusion studies are not well suited for such investigations since they are restricted to short term exposure and term placenta, major advancements in the development of human-based *in vitro* models of the placenta and the maternal-fetal interface have great potential to further exploit the identified toxicity mechanisms and to ultimately achieve a comprehensive understanding on the developmental toxicity of NPs.

CRediT authorship contribution statement

S. Chortarea: Writing – original draft, Visualization, Investigation, Formal analysis, Data curation. **G. Gupta:** Writing – original draft, Investigation, Formal analysis, Writing – review & editing. **L.A. Saarimäki:** Investigation, Formal analysis, Data curation, Writing – review & editing. **W. Netkueakul:** Methodology, Investigation. **P. Manser:** Investigation, Formal analysis. **L. Aengenheister:** Investigation, Formal analysis. **A. Wichser:** Methodology, Investigation. **V. Fortino:** Investigation, Formal analysis, Writing – review & editing. **P. Wick:** Conceptualization, Writing – review & editing, Resources, Project administration, Funding acquisition. **D. Greco:** Conceptualization, Supervision, Writing – review & editing, Resources, Project administration, Funding acquisition. **T. Buerki-Thurnherr:** Conceptualization, Supervision, Writing – original draft, Visualization, Writing – review & editing, Resources, Project administration, Funding acquisition.

Declaration of Competing Interest

The authors declare that they have no known competing financial interests or personal relationships that could have appeared to influence the work reported in this paper.

Data availability

Microarray data associated with this publication have been deposited to the NCBI Gene Expression Omnibus (GEO) database and are accessible through the accession number GSE220756.

Acknowledgement

The research leading to these results has received funding from the Swiss National Science Foundation (grant no 31003A_179337), the European Union 7th Framework Program for Research, Technological Development and Demonstration under grant agreement no 309329 (NANOSOLUTIONS) and the European Union (EU) 8th Framework Program for Research and Technological Development, Graphene Flagship project (H2020-FET-GrapheneCore2 - #785219 and H2020-FET- GrapheneCore3 - #881603). We would like to thank Dr. Alexander Gogos for support with ICP-MS analysis.

Appendix A. Supplementary material

Supplementary data to this article can be found online at https://doi.org/10.1016/j.envint.2023.108015.

References

Abán, C.E., et al., 2018. Crosstalk Between Nitric Oxide and Endocannabinoid Signaling Pathways in Normal and Pathological Placentation. Frontiers in Physiology 9.
Adamcakova-Dodd, A., et al., 2015. Effects of prenatal inhalation exposure to copper nanoparticles on murine dams and offspring. Particle and Fibre Toxicology 12 (1), 30.
Aengenheister, L., et al., 2018. An advanced human in vitro co-culture model for translocation studies across the placental barrier. Scientific Reports 8 (1), 5388.
Aengenheister, L., et al., 2018. Gold nanoparticle distribution in advanced in vitro and ex vivo human placental barrier models. J Nanobiotechnology 16 (1), 79.
Aengenheister, L., et al., 2019. Investigating the accumulation and translocation of titanium dioxide nanoparticles with different surface modifications in static and dynamic human placental transfer models. European Journal of Pharmaceutics and Biopharmaceutics 142, 488–497.
Aengenheister, L., et al., 2021. Research on nanoparticles in human perfused placenta: State of the art and perspectives. Placenta 104, 199–207.
Albrecht, E.D., Pepe, G.J., 2010. Estrogen regulation of placental angiogenesis and fetal ovarian development during primate pregnancy. The International Journal of Developmental Biology 54 (2–3), 397–408.
Angelé-Martínez, C., et al., 2017. Reactive oxygen species generation by copper(II) oxide nanoparticles determined by DNA damage assays and EPR spectroscopy. Nanotoxicology 11 (2), 278–288.
Barua, S., et al., 2014. Increasing maternal or post-weaning folic acid alters gene expression and moderately changes behavior in the offspring. PLoS One1 9 (7), e101674.
Berkane, N., et al., 2017. From Pregnancy to Preeclampsia: A Key Role for Estrogens. Endocrine Reviews 38 (2), 123–144.
Bick, R.L., et al., 1998. Recurrent miscarriage: causes, evaluation, and treatment. Medscape Women's Health 3 (3), 2.
Bongaerts, E., et al., 2022. Maternal exposure to ambient black carbon particles and their presence in maternal and fetal circulation and organs: an analysis of two independent population-based observational studies. Lancet Planet Health 6 (10), e804–e811.

Borkham-Kamphorst, E., et al., 2013. Protective effects of lipocalin-2 (LCN2) in acute liver injury suggest a novel function in liver homeostasis. Biochimica et Biophysica Acta 1832 (5), 660–673.
Boyadzhiev, A., et al., 2021. Impact of copper oxide particle dissolution on lung epithelial cell toxicity: response characterization using global transcriptional analysis. Nanotoxicology 15 (3), 380–399.
Braun, A.E., et al., 2019. "Females Are Not Just 'Protected' Males": Sex-Specific Vulnerabilities in Placenta and Brain after Prenatal Immune Disruption. eNeuro 6 (6).
Braun, T., et al., 2021. Detection of Microplastic in Human Placenta and Meconium in a Clinical Setting. Pharmaceutics 13 (7).
Braun, A.E., et al., 2022. Sex at the interface: the origin and impact of sex differences in the developing human placenta. Biology of Sex Differences 13 (1), 50.
Briffa, J.F., et al., 2015. Leptin in pregnancy and development: a contributor to adulthood disease? American Journal of Physiology-Endocrinology and Metabolism 308 (5), E335–E350.
Bruinink, A., Wang, J., Wick, P., 2015. Effect of particle agglomeration in nanotoxicology. Archives of Toxicology 89 (5), 659–675.
Buckberry, S., et al., 2014. Integrative transcriptome meta-analysis reveals widespread sex-biased gene expression at the human fetal-maternal interface. Molecular Human Reproduction 20 (8), 810–819.
Buerki-Thurnherr, T., et al., 2018. Developmental Toxicity of Nanomaterials: Need for a Better Understanding of Indirect Effects. Chemical Research in Toxicology 31 (8), 641–642.
Buhimschi, I.A., et al., 2014. Protein misfolding, congophilia, oligomerization, and defective amyloid processing in preeclampsia. Science Translational Medicine 6 (245), p. 245ra92.
Burton, G.J., Fowden, A.L., 2015. The placenta: a multifaceted, transient organ. Philosophical Transactions of the Royal Society of London. Series B, Biological Sciences 370 (1663), 20140066.
Busso, D., et al., 2020. Chapter 57 - Nutrients and Gene Expression in Development. In: Caterina, R.D.E., Martinez, J.A., Kohlmeier, M. (Eds.), Principles of Nutrigenetics and Nutrigenomics. Academic Press, pp. 423–430.
Cassat, J.E., Skaar, E.P., 2013. Iron in infection and immunity. Cell Host & Microbe 13 (5), 509–519.
Chan, S.Y., Vasilopoulou, E., Kilby, M.D., 2009. The role of the placenta in thyroid hormone delivery to the fetus. Nature Clinical Practice. Endocrinology & Metabolism 5 (1), 45–54.
Chang, G.W., Kam, P.C., 1999. The physiological and pharmacological roles of cytochrome P450 isoenzymes. Anaesthesia 54 (1), 42–50.
Chen, E.Y., et al., 2013. Enrichr: interactive and collaborative HTML5 gene list enrichment analysis tool. BMC Bioinformatics 14, 128.
Cho, W.-S., et al., 2012. Zeta Potential and Solubility to Toxic Ions as Mechanisms of Lung Inflammation Caused by Metal/Metal Oxide Nanoparticles. Toxicological Sciences 126 (2), 469–477.
Chortarea, S., et al., 2017. Human Asthmatic Bronchial Cells Are More Susceptible to Subchronic Repeated Exposures of Aerosolized Carbon Nanotubes At Occupationally Relevant Doses Than Healthy Cells. ACS Nano 11 (8), 7615–7625.
Chrelias, G., et al., 2016. Serum inhibin and leptin: Risk factors for pre-eclampsia? Clinica Chimica Acta 463, 84–87.
Colombo, G., et al., 2019. Cytotoxic and proinflammatory responses induced by ZnO nanoparticles in in vitro intestinal barrier. Journal of Applied Toxicology 39 (8), 1155–1163.
Cornock, R., et al., 2013. The effect of feeding a low iron diet prior to and during gestation on fetal and maternal iron homeostasis in two strains of rat. Reproductive Biology and Endocrinology 11, 32.
Costa, P.M., et al., 2018. Transcriptional profiling reveals gene expression changes associated with inflammation and cell proliferation following short-term inhalation exposure to copper oxide nanoparticles. Journal of Applied Toxicology 38 (3), 385–397.
Das, S., Baker, A.B., 2016. Biomaterials and Nanotherapeutics for Enhancing Skin Wound Healing. Frontiers in Bioengineering and Biotechnology 4, 82.
Daugaard, M., Rohde, M., Jäättelä, M., 2007. The heat shock protein 70 family: Highly homologous proteins with overlapping and distinct functions. FEBS Letters 581 (19), 3702–3710.
De Falco, S., 2012. The discovery of placenta growth factor and its biological activity. Experimental & Molecular Medicine 44 (1), 1–9.
de Knegt, V.E., et al., 2021. The Role of Leptin in Fetal Growth during Pre-Eclampsia. International Journal of Molecular Sciences 22 (9), 4569.
D'Errico, J.N., et al., 2022. Maternal, placental, and fetal distribution of titanium after repeated titanium dioxide nanoparticle inhalation through pregnancy. Placenta 121, 99–108.
Di Bucchianico, S., et al., 2013. Multiple cytotoxic and genotoxic effects induced in vitro by differently shaped copper oxide nanomaterials. Mutagenesis 28 (3), 287–299.
Díaz, P., Powell, T.L., Jansson, T., 2014. The role of placental nutrient sensing in maternal-fetal resource allocation. Biology of Reproduction 91 (4), 82.
Dugershaw, B.B., et al., 2020. Recent insights on indirect mechanisms in developmental toxicity of nanomaterials. Particle and Fibre Toxicology 17 (1), 31.
Dusza, H.M., et al., 2022. Uptake, Transport, and Toxicity of Pristine and Weathered Micro- and Nanoplastics in Human Placenta Cells. Environmental Health Perspectives 130 (9), 097006.
Duval, M., et al., 2003. Vascular Endothelial Growth Factor-dependent Down-regulation of Flk-1/KDR Involves Cbl-mediated Ubiquitination: CONSEQUENCES ON NITRIC OXIDE PRODUCTION FROM ENDOTHELIAL CELLS*. Journal of Biological Chemistry 278 (22), 20091–20097.
Fan, Y., Kang, Y., Zhang, M., 2016. A meta-analysis of copper level and risk of preeclampsia: evidence from 12 publications. Bioscience Reports 36 (4).
Farias, P.M., et al., 2020. Minerals in Pregnancy and Their Impact on Child Growth and Development. Molecules 25 (23).
Fleischer, N.L., et al., 2014. Outdoor air pollution, preterm birth, and low birth weight: analysis of the world health organization global survey on maternal and perinatal health. Environmental Health Perspectives 122 (4), 425–430.
Fournier, S.B., et al., 2020. Nanopolystyrene translocation and fetal deposition after acute lung exposure during late-stage pregnancy. Particle and Fibre Toxicology 17 (1), 55.
Fröhlich, E., et al., 2010. Size-dependent effects of nanoparticles on the activity of cytochrome P450 isoenzymes. Toxicology and Applied Pharmacology 242 (3), 326–332.
Furer, L.A., et al., 2022. Novel electrospun chitosan/PEO membranes for more predictive nanoparticle transport studies at biological barriers. Nanoscale 14 (33), 12136–12152.
Future Markets Inc., The global market for copper oxide nanoparticles, 2010-2025. Available at: http://www.futuremarketsinc.com/global-market-copper-oxide-nanoparticles-2010-2025.
Gabay, C., 2006. Interleukin-6 and chronic inflammation. Arthritis Research & Therapy 8 (2), S3.
Gigante, B., et al., 2006. Plgf-/-eNos-/- mice show defective angiogenesis associated with increased oxidative stress in response to tissue ischemia. The FASEB Journal 20 (7), 970–972.
Gnanavel, V., Palanichamy, V., Roopan, S.M., 2017. Biosynthesis and characterization of copper oxide nanoparticles and its anticancer activity on human colon cancer cell lines (HCT-116). Journal of Photochemistry and Photobiology. B 171, 133–138.
Grafmueller, S., et al., 2013. Determination of the Transport Rate of Xenobiotics and Nanomaterials Across the Placenta using the ex vivo Human Placental Perfusion Model. Journal of Visualized Experiments 76, e50401.
Grafmueller, S., et al., 2015. Bidirectional Transfer Study of Polystyrene Nanoparticles across the Placental Barrier in an Human Placental Perfusion Model. Environmental Health Perspectives.
Grafmueller, S., et al., 2015. Transfer studies of polystyrene nanoparticles in the ex vivo human placenta perfusion model: key sources of artifacts. Science and Technology of Advanced Materials 16 (4), 044602.
Greenberg, J.A., et al., 2011. Folic Acid supplementation and pregnancy: more than just neural tube defect prevention. Reviews in Obstetrics and Gynecology 4 (2), 52–59.
Grigore, M.E., et al., 2016. Methods of Synthesis, Properties and Biomedical Applications of CuO Nanoparticles. Pharmaceuticals (Basel) 9 (4).
Gruber, M.M., et al., 2020. Plasma proteins facilitates placental transfer of polystyrene particles. Journal of Nanobiotechnology 18 (1), 128.
Gunshin, H., et al., 2005. Slc11a2 is required for intestinal iron absorption and erythropoiesis but dispensable in placenta and liver. The Journal of Clinical Investigation 115 (5), 1258–1266.
Gupta, G., et al., 2022. Copper oxide nanoparticles trigger macrophage cell death with misfolding of Cu/Zn superoxide dismutase 1 (SOD1). Particle and Fibre Toxicology 19 (1), 33.
Hesler, M., et al., 2019. Multi-endpoint toxicological assessment of polystyrene nano- and microparticles in different biological models in vitro. Toxicology in Vitro 61, 104610.
Hoffman, D.J., Reynolds, R.M., Hardy, D.B., 2017. Developmental origins of health and disease: current knowledge and potential mechanisms. Nutrition Reviews 75 (12), 951–970.
Honarvar, Z., Hadian, Z., Mashayekh, M., 2016. Nanocomposites in food packaging applications and their risk assessment for health. Electronic Physician 8 (6), 2531–2538.
Hop, H.T., et al., 2018. Lipocalin 2 (Lcn2) interferes with iron uptake by Brucella abortus and dampens immunoregulation during infection of RAW 264.7 macrophages. Cellular Microbiology 20 (3).
Horvatits, T., et al., 2022. Microplastics detected in cirrhotic liver tissue. eBioMedicine 82.
Huang, X., et al., 2014. The genotype-dependent influence of functionalized multiwalled carbon nanotubes on fetal development. Biomaterials 35 (2), 856–865.
Hwang, J., et al., 2020. Potential toxicity of polystyrene microplastic particles. Scientific Reports 10 (1), 7391.
Jenner, L.C., et al., 2022. Detection of microplastics in human lung tissue using muFTIR spectroscopy. The Science of the Total Environment 831, 154907.
Jing, X., et al., 2015. Toxicity of copper oxide nanoparticles in lung epithelial cells exposed at the air-liquid interface compared with in vivo assessment. Toxicology In Vitro 29 (3), 502–511.
Jurado, S., et al., Maternal and Fetal Complications Due to Decreased Nitric Oxide Synthesis during Gestation, in Complications of Pregnancy, A. Hassan, Editor. 2019, IntechOpen: Rijeka. p. Ch. 6.
Kaartokallio, T., et al., 2015. Gene expression profiling of pre-eclamptic placentae by RNA sequencing. Scientific Reports 5, 14107.
Kamyshny, A., Magdassi, S., 2014. Conductive nanomaterials for printed electronics. Small 10 (17), 3515–3535.
Karlsson, H.L., et al., 2008. Copper oxide nanoparticles are highly toxic: a comparison between metal oxide nanoparticles and carbon nanotubes. Chemical Research in Toxicology 21 (9), 1726–1732.
Kashif, M., et al., 2012. Nuclear Factor Erythroid-derived 2 (Nfe2) Regulates JunD DNA-binding Activity via Acetylation: A NOVEL MECHANISM REGULATING TROPHOBLAST DIFFERENTIATION*. Journal of Biological Chemistry 287 (8), 5400–5411.

Kinaret, P., et al., 2017. Inhalation and Oropharyngeal Aspiration Exposure to Rod-Like Carbon Nanotubes Induce Similar Airway Inflammation and Biological Responses in Mouse Lungs. ACS Nano 11 (1), 291–303.
Klębowski, B., et al., 2018. Applications of Noble Metal-Based Nanoparticles in Medicine. International Journal of Molecular Sciences 19 (12).
Kooter, I., et al., 2019. Molecular Signature of Asthma-Enhanced Sensitivity to CuO Nanoparticle Aerosols from 3D Cell Model. ACS Nano 13 (6), 6932–6946.
Krause, B.J., Hanson, M.A., Casanello, P., 2011. Role of nitric oxide in placental vascular development and function. Placenta 32 (11), 797–805.
Kumazaki, K., et al., 2002. Expression of vascular endothelial growth factor, placental growth factor, and their receptors Flt-1 and KDR in human placenta under pathologic conditions. Human Pathology 33 (11), 1069–1077.
Labib, S., et al., 2016. Nano-risk Science: application of toxicogenomics in an adverse outcome pathway framework for risk assessment of multi-walled carbon nanotubes. Particle and Fibre Toxicology 13 (1), 15.
Lai, X., et al., 2018. Intranasal Delivery of Copper Oxide Nanoparticles Induces Pulmonary Toxicity and Fibrosis in C57BL/6 mice. Scientific Reports 8 (1), 4499.
Landsiedel, R., et al., 2010. Testing metal-oxide nanomaterials for human safety. Advanced Materials 22 (24), 2601–2627.
Leek, J.T., et al., 2012. The sva package for removing batch effects and other unwanted variation in high-throughput experiments. Bioinformatics 28 (6), 882–883.
Lehner, R., et al., 2019. Emergence of Nanoplastic in the Environment and Possible Impact on Human Health. Environmental Science & Technology 53 (4), 1748–1765.
Leslie, H.A., et al., 2022. Discovery and quantification of plastic particle pollution in human blood. Environment International 163, 107199.
Luo, J., et al., 2020. Oral exposure of pregnant rats to copper nanoparticles caused nutritional imbalance and liver dysfunction in fetus. Ecotoxicology and Environmental Safety 206, 111206.
Mackenzie, R.M., et al., 2012. Endothelial FOS expression and pre-eclampsia. BJOG : An International Journal of Obstetrics and Gynaecology 119 (13), 1564–1571.
Mahler, G.J., et al., 2012. Oral exposure to polystyrene nanoparticles affects iron absorption. Nature Nanotechnology 7 (4), 264–271.
Marchesan, S., Prato, M., 2013. Nanomaterials for (Nano)medicine. ACS Medicinal Chemistry Letters 4 (2), 147–149.
Marshall, N.E., et al., 2022. The importance of nutrition in pregnancy and lactation: lifelong consequences. American Journal of Obstetrics and Gynecology 226 (5), 607–632.
Marwah, V.S., et al., 2018. INfORM: Inference of NetwOrk Response Modules. Bioinformatics 34 (12), 2136–2138.
Marwah, V.S., et al., 2019. eUTOPIA: solUTion for Omics data PreprocessIng and Analysis. Source Code for Biology and Medicine 14, 1.
Marzioni, D., et al., 2010. Activating protein-1 family of transcription factors in the human placenta complicated by preeclampsia with and without fetal growth restriction. Placenta 31 (10), 919–927.
Meakin, A.S., et al., 2021. Let's Talk about Placental Sex, Baby: Understanding Mechanisms That Drive Female- and Male-Specific Fetal Growth and Developmental Outcomes. International Journal of Molecular Sciences 22 (12).
Midander, K., et al., 2009. Surface characteristics, copper release, and toxicity of nano- and micrometer-sized copper and copper(II) oxide particles: a cross-disciplinary study. Small 5 (3), 389–399.
Miehle, K., Stepan, H., Fasshauer, M., 2012. Leptin, adiponectin and other adipokines in gestational diabetes mellitus and pre-eclampsia. Clinical Endocrinology 76 (1), 2–11.
Mohammadi, S., et al., 2021. Assessing donor-to-donor variability in human intestinal organoid cultures. Stem Cell Reports 16 (9), 2364–2378.
Moreno-Olivas, F., Tako, E., Mahler, G.J., 2019. ZnO nanoparticles affect nutrient transport in an in vitro model of the small intestine. Food and Chemical Toxicology 124, 112–127.
Mousa, A., Naqash, A., Lim, S., 2019. Macronutrient and Micronutrient Intake during Pregnancy: An Overview of Recent Evidence. Nutrients 11 (2).
Muoth, C., et al., 2016. A 3D co-culture microtissue model of the human placenta for nanotoxicity assessment. Nanoscale.
Nairz, M., et al., 2015. Iron Regulatory Proteins Mediate Host Resistance to Salmonella Infection. Cell Host & Microbe 18 (2), 254–261.
Napso, T., et al., 2018. The Role of Placental Hormones in Mediating Maternal Adaptations to Support Pregnancy and Lactation. Frontiers in Physiology 9, 1091.
Naugler, W.E., Karin, M., 2008. The wolf in sheep's clothing: the role of interleukin-6 in immunity, inflammation and cancer. Trends in Molecular Medicine 14 (3), 109–119.
Nobile, S., Di Sipio Morgia, C., Vento, G., 2022. Perinatal Origins of Adult Disease and Opportunities for Health Promotion. A Narrative Review. J Pers Med 12 (2).
Notter, T., et al., 2018. Prenatal exposure to TiO2 nanoparticles in mice causes behavioral deficits with relevance to autism spectrum disorder and beyond. Translational Psychiatry 8 (1), 193.
Oliveros, J.C. Venny. An interactive tool for comparing lists with Venn's diagrams.; Available from: https://bioinfogp.cnb.csic.es/tools/venny/index.html.
Paquette, A., et al., 2018. Temporal transcriptomic analysis of metabolic genes in maternal organs and placenta during murine pregnancy†. Biology of Reproduction 99 (6), 1255–1265.
Paul, E., et al., 2017. Pulmonary exposure to metallic nanomaterials during pregnancy irreversibly impairs lung development of the offspring. Nanotoxicology 11 (4), 484–495.
Pérez-Pérez, A., et al., 2018. Leptin action in normal and pathological pregnancies. Journal of Cellular and Molecular Medicine 22 (2), 716–727.
Plastics Europe. Plastics-the facts 2018. An analysis of European plastics production, demand and waste data. Available from: https://plasticseurope.org/wp-content/uploads/2021/10/2018-Plastics-the-facts.pdf.
Prietl, B., et al., 2014. Nano-sized and micro-sized polystyrene particles affect phagocyte function. Cell Biology and Toxicology 30 (1), 1–16.
Prins, J.R., Gomez-Lopez, N., Robertson, S.A., 2012. Interleukin-6 in pregnancy and gestational disorders. Journal of Reproductive Immunology 95 (1), 1–14.
Ragusa, A., et al., 2021. Plasticenta: First evidence of microplastics in human placenta. Environment International 146, 106274.
Ragusa, A., et al., 2022. Deeply in Plasticenta: Presence of Microplastics in the Intracellular Compartment of Human Placentas. International Journal of Environmental Research and Public Health 19 (18).
Raj, S., et al., 2012. Nanotechnology in cosmetics: Opportunities and challenges. Journal of Pharmacy & Bioallied Sciences 4 (3), 186–193.
Rashidi, L., Khosravi-Darani, K., 2011. The applications of nanotechnology in food industry. Critical Reviews in Food Science and Nutrition 51 (8), 723–730.
Redman, C.W., Sargent, I.L., 2005. Latest advances in understanding preeclampsia. Science 308 (5728), 1592–1594.
Renaud, S.J., et al., 2014. The FOS Transcription Factor Family Differentially Controls Trophoblast Migration and Invasion*. Journal of Biological Chemistry 289 (8), 5025–5039.
Ritchie, M.E., et al., 2015. limma powers differential expression analyses for RNA-sequencing and microarray studies. Nucleic Acids Research 43 (7), e47.
Rumer, K.K., et al., 2013. Siglec-6 expression is increased in placentas from pregnancies complicated by preterm preeclampsia. Reproductive Sciences 20 (6), 646–653.
Sangkhae, V., et al., 2020. Effects of maternal iron status on placental and fetal iron homeostasis. The Journal of Clinical Investigation 130 (2), 625–640.
Saporito-Magriñá, C.M., et al., 2018. Copper-induced cell death and the protective role of glutathione: the implication of impaired protein folding rather than oxidative stress†. Metallomics 10 (12), 1743–1754.
Sarkar, A., et al., 2011. Nano-copper induces oxidative stress and apoptosis in kidney via both extrinsic and intrinsic pathways. Toxicology 290 (2–3), 208–217.
Scala, G., et al., 2019. FunMappOne: a tool to hierarchically organize and visually navigate functional gene annotations in multiple experiments. BMC Bioinformatics 20 (1), 79.
Schmittgen, T.D., Livak, K.J., 2008. Analyzing real-time PCR data by the comparative CT method. Nature Protocols 3 (6), 1101–1108.
Schwabl, P., et al., 2019. Detection of Various Microplastics in Human Stool: A Prospective Case Series. Annals of Internal Medicine 171 (7), 453–457.
Sedlmeier, E.-M., et al., 2014. Human placental transcriptome shows sexually dimorphic gene expression and responsiveness to maternal dietary n-3 long-chain polyunsaturated fatty acid intervention during pregnancy. BMC Genomics 15 (1), 941.
Shirasuna, K., et al., 2015. Nanosilica-induced placental inflammation and pregnancy complications: Different roles of the inflammasome components NLRP3 and ASC. Nanotoxicology 9 (5), 554–567.
Sõber, S., et al., 2015. Extensive shift in placental transcriptome profile in preeclampsia and placental origin of adverse pregnancy outcomes. Scientific Reports 5 (1), 13336.
Song, X., et al., 2017. High serum copper level is associated with an increased risk of preeclampsia in Asians: A meta-analysis. Nutrition Research 39, 14–24.
Song, H., W. Ludovic, and C. Samuel, The Use of In Vitro 3D Cell Models in Drug Development for Respiratory Diseases, in Drug Discovery and Development, M.K. Izet, Editor. 2011, IntechOpen: Rijeka. p. Ch. 8.
Sood, R., et al., 2006. Gene expression patterns in human placenta. Proceedings of the National Academy of Sciences of the United States of America 103 (14), 5478–5483.
Strauch, B.M., et al., 2017. Comparison between micro- and nanosized copper oxide and water soluble copper chloride: interrelationship between intracellular copper concentrations, oxidative stress and DNA damage response in human lung cells. Particle and Fibre Toxicology 14 (1), 28.
Szklarczyk, D., et al., 2017. The STRING database in 2017: quality-controlled protein-protein association networks, made broadly accessible. Nucleic Acids Research 45 (D1), D362–D368.
Tao, Q., et al., 2001. Kinase Insert Domain Receptor (KDR) Extracellular Immunoglobulin-like Domains 4–7 Contain Structural Features That Block Receptor Dimerization and Vascular Endothelial Growth Factor-induced Signaling*. Journal of Biological Chemistry 276 (24), 21916–21923.
Tarasova, N.K., et al., 2017. Cytotoxic and Proinflammatory Effects of Metal-Based Nanoparticles on THP-1 Monocytes Characterized by Combined Proteomics Approaches. Journal of Proteome Research 16 (2), 689–697.
Thompson, L.P., et al., 2016. Placental Hypoxia During Early Pregnancy Causes Maternal Hypertension and Placental Insufficiency in the Hypoxic Guinea Pig Model1. Biology of Reproduction 95 (6).
Tikvica, A., et al., 2008. Nitric oxide synthesis in placenta is increased in intrauterine growth restriction and fetal hypoxia. Collegium Antropologicum 32 (2), 565–570.
Tsvetkov, P., et al., 2022. Copper induces cell death by targeting lipoylated TCA cycle proteins. Science 375 (6586), 1254–1261.
Tudisco, L., et al., 2017. Hypoxia activates placental growth factor expression in lymphatic endothelial cells. Oncotarget 8 (20), 32873–32883.
Vidmar, J., et al., 2018. Translocation of silver nanoparticles in the ex vivo human placenta perfusion model characterized by single particle ICP-MS. Nanoscale 10 (25), 11980–11991.
Walker, L.R., Rattigan, M., Canterino, J., 2011. A case of isolated elevated copper levels during pregnancy. Journal of Pregnancy 2011, 385767.
Wang, F., et al., 2020. Molecular mechanisms underlying altered neurobehavioural development of female offspring of mothers with polycystic ovary syndrome: FOS-mediated regulation of neurotrophins in placenta. eBioMedicine 60, 102993.
Wick, P., et al., 2010. Barrier capacity of human placenta for nanosized materials. Environmental Health Perspectives 118 (3), 432–436.

World Health Organization, 1998. Copper Environmental Health Criteria 200. International Programme on Chemical Safety. WHO, Geneva.
Wu, W.L., et al., 2017. The placental interleukin-6 signaling controls fetal brain development and behavior. Brain, Behavior, and Immunity 62, 11–23.
Yamashita, K., et al., 2011. Silica and titanium dioxide nanoparticles cause pregnancy complications in mice. Nature Nanotechnology 6 (5), 321–328.
Yan, Z., et al., 2022. Analysis of Microplastics in Human Feces Reveals a Correlation between Fecal Microplastics and Inflammatory Bowel Disease Status. Environmental Science & Technology 56 (1), 414–421.
Zhang, C.H., et al., 2018. Copper Nanoparticles Show Obvious in vitro and in vivo Reproductive Toxicity via ERK Mediated Signaling Pathway in Female Mice. International Journal of Biological Sciences 14 (13), 1834–1844.
Zhang, L., et al., 2018. Gestational exposure to titanium dioxide nanoparticles impairs the placentation through dysregulation of vascularization, proliferation and apoptosis in mice. International Journal of Nanomedicine 13, 777–789.
Zhang, J., et al., 2021. Occurrence of Polyethylene Terephthalate and Polycarbonate Microplastics in Infant and Adult Feces. Environmental Science & Technology Letters 8 (11), 989–994.
Zheng, Q., et al., 2018. AP1 mediates uPA/uPAR induced FUT4 expression and trophoblast invasion. Journal of Cellular Biochemistry 119 (8), 6442–6451.